

https://dspace.org/

Carbonsupported catalysts for carbon dioxide methanation A review

A Gamal; Khouloud Jlassi; Yahia Ahmad; Mengqi Tang; Siham Al-Qaradawi ...

https://hdl.handle.net/10539/41569
WOS

Downloaded from a DSpace repository. https://dspace.org/

Journal of CO2 Utilization 85 (2024) 102881

Contents lists available at ScienceDirect

Journal of CO2 Utilization

journal homepage: www.elsevier.com/locate/jcou

Review Article

Carbon-supported catalysts for carbon dioxide methanation: A review

Ahmed Gamal [a,d], Khouloud Jlassi [a,*], Yahia H. Ahmad [b], Mengqi Tang [c], Siham Y. Al-Qaradawi [b], Mohamed M. Chehimi [c,*], Kenneth I. Ozoemena [d,*], Aboubakr M. Abdullah [a,*]

[a] Center for Advanced Materials, Qatar University, Doha 2713, Qatar
[b] College of Arts and Science, Qatar University, Doha 2713, Qatar
[c] Université Paris Cité, CNRS, ITODYS (UMR 7086), Paris 75013, France
[d] Molecular Sciences Institute, School of Chemistry, University of the Witwatersrand, Private Bag 3, PO Wits, Johannesburg 2050, South Africa

ARTICLE INFO

Keywords:
CO_2 methanation
Carbon-supported catalysts
Graphene
Biochar
Carbon nanotubes

ABSTRACT

Carbon-based materials have attracted significant attention in various catalytic applications. However, they are rarely reported for high-temperature catalytic reactions, owing to their limited thermal stability compared to other common materials such as silica and alumina, especially in oxidation reactions. CO_2 methanation became a pivotal research hotspot due to its ability to contribute to greenhouse gas mitigation. In addition, CO_2 methanation reactions can be carried out below 400 °C in a hydrogen atmosphere, which suits the thermal stability of many modified carbon materials. However, the number of reviews on CO_2 methanation does not match the huge number of the experimental publications on CO_2 methanation particularly reviews on carbon-supported catalysts. Motivated by the paucity of literature, including reviews on carbon-supported catalysts for CO_2 methanation, this review is focused on the catalytic performance of the carbon-supported catalysts of CO_2 methanation. It offers significant comparisons among all reported carbon-supported catalysts, providing a comprehensive study on the effect of the carbonaceous supports, such as graphene, biochar, and carbon nanotubes on the catalytic activity. In addition, it investigates the impact of promoters on the catalytic performance of the carbon-supported catalysts in CO_2 methanation and highlights the preparation methods and their optimized metal compositions that lead to the highest activity and selectivity. We conclude with a brief synopsis on the current challenges and perspectives on the future directions. This study paves the way for broader usage of carbon-supported catalysts for different thermal catalytic applications, not limited to CO_2 methanation.

1. Introduction

Excessive usage of fossil fuels as main energy resources resulted in detrimental carbon dioxide (CO_2) emissions, which are the main reason for global warming. Therefore, the frontlines in science and engineering are persuaded to solve this issue using different strategies such as CO_2 capture and utilization [1]. One of the most promising reactions of CO_2 utilization is CO_2 hydrogenation to methane (Eq. (1)) or to methanol (Eq. (2)) [2]. However, the path of CO_2 hydrogenation to methanol necessitates harsh operating parameters such as high reaction temperatures and high applied pressures [3]. On the other hand, CO_2 hydrogenation to methane does not require high operating temperatures and can be operated at atmospheric pressure. Thus, CO_2 methanation has attracted researchers in the last decade to explore it intensively, which is evidenced by the significant increase in the number of publications on CO_2 methanation in the last ten years (Fig. 1).

$$CO_2 + 4H_2 \rightarrow CH_4 + 2H_2O\ \Delta H_{298K} = -165\ kJ/mol;\ \Delta G = -141.9\ kJ/mol \quad (1)$$

$$CO_2 + 3H_2 \rightleftharpoons CH_3OH + H_2O\ \Delta H_{298K} = -49.5\ kJ/mol;\ \Delta G = 3.5\ kJ/mol \quad (2)$$

Both noble and transition metals such as Ru and Ni were reported as catalysts for CO_2 methanation, with different supports such as silica [4] and alumina [5]. In contrast, carbon based catalysts are not favored in the thermal catalytic reactions due to their thermal instability, particularly in the high-temperature regime and oxidation reactions [6].

* Corresponding authors.
E-mail addresses: Khouloud.jlassi@qu.edu.qa (K. Jlassi), mmchehimi@yahoo.fr (M.M. Chehimi), kenneth.ozoemena@wits.ac.za (K.I. Ozoemena), bakr@qu.edu.qa (A.M. Abdullah).

https://doi.org/10.1016/j.jcou.2024.102881
Received 26 May 2024; Received in revised form 10 July 2024; Accepted 16 July 2024
Available online 1 August 2024
2212-9820/© 2024 The Authors. Published by Elsevier Ltd. This is an open access article under the CC BY-NC license (http://creativecommons.org/licenses/by-nc/4.0/).

However, CO_2 methanation reactions can be operated below 400 °C in hydrogen atmosphere, which meets with the thermal stability of different modified carbon materials.

Recently, researchers have become more interested in investigating carbon-supported catalysts for CO_2 methanation to achieve a sustainable catalyst for the environmentally friendly reaction (CO_2 methanation), which is indicated by the increasing number of publications in the last five years (Fig. 1a). However, there is still a big gap between the number of reported articles on CO_2 methanation and the reported carbon-supported catalysts used for CO_2 methanation. This is despite the interest of carbon catalysts or carbon supports, as discussed by Figueiredo et al. [7]. The authors reported an interest in carbon as materials with controlled porous structure and active oxygen surface sites, introduced by *e.g.* surface oxidation. On ceramics, oxygen sites can bridge the CO intermediate before the formation of bidentate formate, and methane [8]. Oxygen vacancies could be created due to the reducing effect of hydrogen during the process, and are known as active sites to host CO_2 [8]. Carbon materials such as carbon nanotubes could be partially oxidized, but activated carbon and biochar have the advantage of containing nitrogen sites that are not borne by ceramics. Such nitrogen sites could play a major role in carbon dioxide methanation. They arise from the biomass (biomass protein, chitin, chitosan, …) or could be introduced by doping carbon, therefore resulting in basic nitrogen sites (for example pyridinic nitrogen sites) [9]. It is thus clear that carbon has other features to offer compared to ceramics and this is what motivated the growing number of investigations of CO_2 methanation over carbon supports.

As shown in Table 1, various reviews were published on the CO_2 methanation discussing its proposed mechanisms [10,11], the catalytic performance of the reported catalysts [12–14], the effect of supports and promoters [15], the preparation methods and reaction conditions [16], mechanisms and thermodynamics [17]. However, reported reviews on CO_2 methanation remain scarce compared to the increasing number of publications on that topic. In addition, only one review is reported on the carbon-supported catalysts [17], which mainly focused on the CO_2 hydrogenation to methanol in addition to the thermodynamics and mechanisms. Thus, we provide a vital review on the state-of-the-art of carbon-supported catalysts reported for the thermal catalytic CO_2 methanation. This review focuses on the catalytic performance of the carbon-supported catalysts, providing significant comparisons among all reported catalysts. It provides insight into how carbonaceous support influences catalysts and identifies which type of carbon is more advantageous. It also examines the influence of promoters on the catalytic efficiency of carbon-supported catalysts in CO_2 methanation. Furthermore, it discusses various preparation techniques and their optimized metal compositions, as well as delving into the resulting catalytic activity of these carbon-supported catalysts. We will finish by stressing the up-to-date challenges and perspectives in the field. This review paves the way for wider utilization of carbon-supported catalysts in CO_2 methanation, and more generally in thermo-catalytic processes.

Table 1
Summary of the most relevant reviews on CO_2 methanation.

Title	Focus	Ref
Progress in reaction mechanisms and catalyst development of ceria-based catalysts for low-temperature CO_2 methanation	perspectives on understanding the active sites and intermediates' evolution on Ceria-based catalysts	[10]
Catalysis mechanisms of CO_2 and CO methanation	Only on the fundamentals of reaction mechanisms of CO_2 and CO methanation	[11]
Recent advances in thermal catalytic CO_2 methanation on hydrotalcite-derived catalysts	hydrotalcite-derived systems and their catalytic performance in CO_2 methanation	[12]
Research Progress and Reaction Mechanism of CO_2 Methanation over Ni-Based Catalysts at Low Temperature: A Review	Nature of active sites, supports, promoters, and preparation methods of Ni-based catalysts, reported for the CO_2 methanation	[13]
Recent trend in thermal catalytic low temperature CO_2 methanation: A critical review	Reaction kinetics, catalyst's supports, promoters, and reactor technologies	[14]
Supported catalysts for CO_2 methanation: A review	Focusing on the catalyst deactivation and catalyst promoters	[15]
Recent Progresses in Constructing the Highly Efficient Ni Based Catalysts With Advanced Low-Temperature Activity Toward CO_2 Methanation	Catalytic supports, catalytic dopants, preparation methods, and reaction conditions	[16]
Bimetallic Ni-based catalysts for CO_2 methanation: A review	Evaluation of catalytic performance of other transition and noble metals attached to Ni as bimetallic catalysts such as Fe, Co, Cu, Ru, Rh, Pt, and Pd	[18]
The role of alkali and alkaline earth metals in the CO_2 methanation reaction and the combined capture and methanation of CO_2	Catalytic performance of alkali and alkaline earth metals and the developments of dual-function materials (DFMs)	[19]
Recent Advancements, Fundamental Challenges, and Opportunities in Catalytic Methanation of CO_2	Discussing the reaction mechanism, catalytic materials, and novel combination of metal active phase and its synergy.	[20]
CO_2 Hydrogenation to Methanol and Methane over Carbon-Supported Catalysts	Thermodynamics and mechanisms of CO_2 hydrogenation over ceramic and carbon supports.	[17]
Carbon Dioxide Methanation Enabled by Biochar-Nanocatalyst Composite Materials: A Mini-Review	Focusing on the biochar as a support for the metal-based catalysts reported for the CO_2 methanation.	[21]

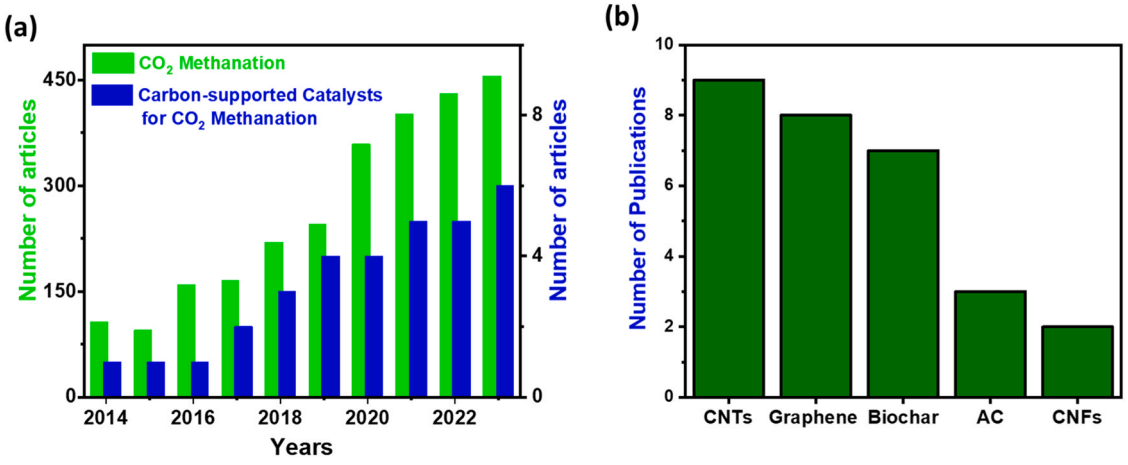


Fig. 1. (a) Publications number of CO_2 methanation in the last decade, and (b) Publications number of the reported carbon supports for the CO_2 methanation. Data obtained from Web of Science, until December 2023.

2. Carbon supports

Various types of carbon were studied as supports for the catalysts of CO_2 methanation such as graphene, carbon nanotubes (CNTs), and biochar. In addition, few articles were reported on the activated carbon (AC) and carbon nanofibers (CNFs) as supports, as shown in Fig. 1b, which shows the number of publications of the different reported carbon types as supports for the catalysts of CO_2 methanation, according to Web of Science. Moreover, effect of reported promoters and N-doped carbonaceous supports are studied as well.

3. Carbon nanotube supports (CNTs)

In the last decades, carbon nanotubes (CNTs) triggered increased research interest owing to their exceptional properties, such as large specific surface area, high electrical and thermal conductivities, and enhanced mechanical properties [22]. The unique tubular structure of CNT can enhance the dispersion of the active components via confinement effect that can restrict their particle size down to the nanometer scale and prevent their migration and agglomeration [23]. In addition, the unique structure and good electrical conductivity of CNT can boost the interaction with reactant molecules and favor the electron transfer between the active sites and the reactants [24]. Suslova et al. [25]. studied the hydrogenation of CO_2 on cobalt-based catalysts supported on different types of synthesized carbon supports, *i.e.* carbon nanotubes (CNTs), carbon nanofibers, few-layer graphite fragments compared to alumina support.

Carbon nanotubes (CNTs) were prepared by hexane pyrolysis at 750 °C in the presence of MgO under a flow of N_2 as a carrier gas, carbon nanofibers (CNFs) were synthesized by the pyrolysis of benzene containing Fe(acac)3, while few-layer graphite (FLG) fragments were prepared via pyrolysis of butylamine in the presence of MgO at 900 °C [25]. CNTs–Al_2O_3 composites were prepared via methane pyrolysis at 650 °C for 5 h in the presence of Al_2O_3. The CNTs surface was functionalized by treating with concentrated nitric acid. CNTs and FLG fragments were thermally stable up to 570–650 °C, while CNFs is distructed above 300 °C [25]. The reaction product was CO, CH_4 or a mixture of them depending on the nature of support material, the cobalt size, cobalt loading and the cobalt phase. The results showed that the Co/CNTs catalysts containing less than 5 wt% Co are inactive owing to the amorphism of the metal. It was also found that the functionalization of the surface of CNTs with carboxy groups or the introduction of nitrogen atoms into FLG enhances the stability of the cobalt-containing catalysts. Ni-supported Ce-promoted CNTs was synthesized by ultrasonic-assisted impregnation and investigated as catalyst for CO_2 methanation compared to non-promoted and alumina-supported catalysts [26]. The results showed that the insertion of cerium improved the dispersion of Ni, enhanced the reducibility of NiO and boosted the CO_2 activation. In addition, the confinement effect of CNTs prevented the migration and sintering of Ni and retarded the carbon deposition. The CO_2 conversion increased with increasing the cerium loading till 4.5 wt%, owing to the change in the interactions between the active species with the CNTs support and modifying the electronic structure of the active species [26] (see Fig. 2a-b).

At higher Ce contents, no obvious change in CO_2 conversion was observed, due to the coverage of active sites on the surface of the catalyst and the limited capacity of cerium surface to donate electrons to the metallic nickel and adsorbed reactants on the surface of the catalyst [26]. The 12Ni4.5Ce/CNT revealed higher CO_2 conversion (82.5 %), better stability and higher CH_4 selectivity (almost 100 %) after 100 hours compared to 12Ni/CNT catalyst (Fig. 2c). In addition, the Ce-promoted catalyst depicted lower apparent activation energy (13.1 kJ mol^{-1}) compared to the non-promoted catalyst (84.8 kJ mol^{-1}), which might be attributed to the electronic effect as the promoted catalyst could alter the electronic structure of the reactants, making them more reactive [26].

Ni-ZrO_2 catalyst supported on carbon nanotubes was investigated towards CO_2 methanation reaction [27]. The catalyst was synthesized via two different approaches, i.e., sequential impregnation (Ni/Zr/CNT-SEQ) and co-impregnation (Ni/Zr/CNT-COI). The H_2-TPR profile (Fig. 3a) shows that Ni/Zr/CNT-SEQ and Ni/CNT have similar profiles with a strong signal at about 350–400 °C, assigned to weakly interacting NiO with the support, and a weak signal at 500–550 °C, attributed to NiO with intimate contact with the CNTs walls [27]. On the other hand, Ni/Zr/CNT-COI showed a very weak signal at about 326 °C and an intense signal at higher temperatures than Ni/CNT and Ni/Zr/CNT−SEQ. This is an indication that in Ni/Zr/CNT-COI Ni was not easily accessible, as it is mostly covered/blocked by zirconia. Ni/CNT-COI and Ni/Zr/CNT-SEQ revealed similar CO_2 desorption profiles, however, Ni/Zr/CNT-SEQ depicted greater CO_2 adsorption capacity than Ni/Zr/CNT-COI (Fig. 3b). Ni/Zr/CNT-SEQ exhibited higher CO_2 conversion than Ni/Zr/CNT-COI. For example, T10 and T50 values for Ni/Zr/CNT-SEQ were 254 and 369 °C, respectively; however, their values in case of Ni/Zr/CNT-COI were 310 and 500 °C, respectively.

In terms of CH_4 selectivity, Ni/CNT afforded 25–30 % at all temperatures. Meanwhile, Ni/Zr/CNT-COI presented CH_4 selectivity 100 % at 225 °C, which decreased to 16 % at 500 °C. Ni/Zr/CNT-SEQ showed CH_4 selectivity of 100 % up to 450 °C, and then decreased to 79 % at 500 °C (Fig. 3c-d) [27]. The enhanced catalytic activity of Ni/Zr/CNT-SEQ can be attributed to that the Ni-ZrO_2 interface is more accessible to

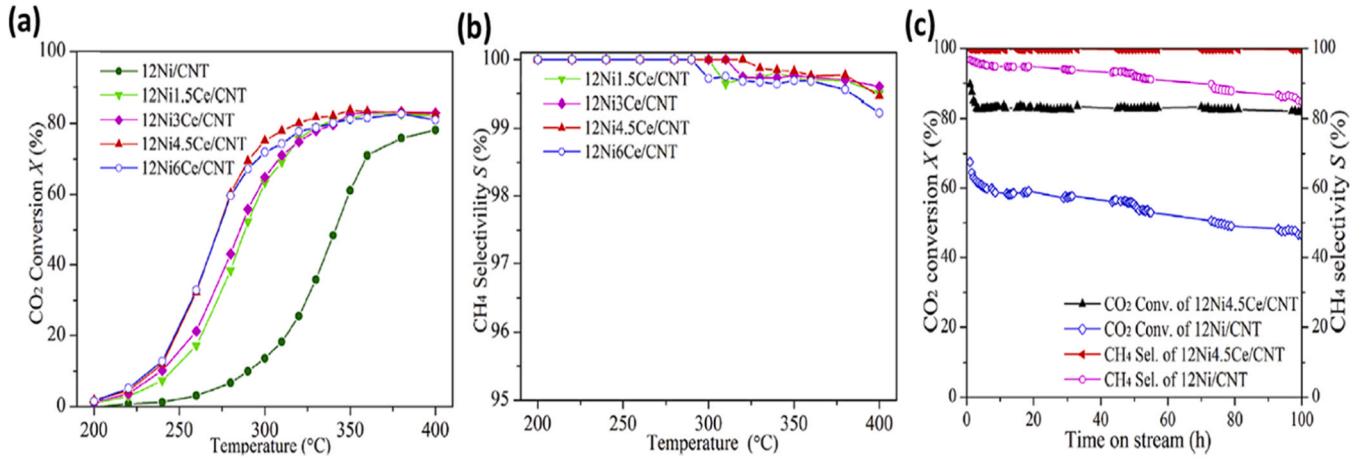


Fig. 2. (a) CO_2 conversion, (b) CH_4 selectivity as a function of temperature for different catalysts, and (c) The stability and CH_4 selectivity of 12Ni/CNT compared to 12Ni4.5Ce/CNT. Reproduced from [26] with permission of Elsevier.

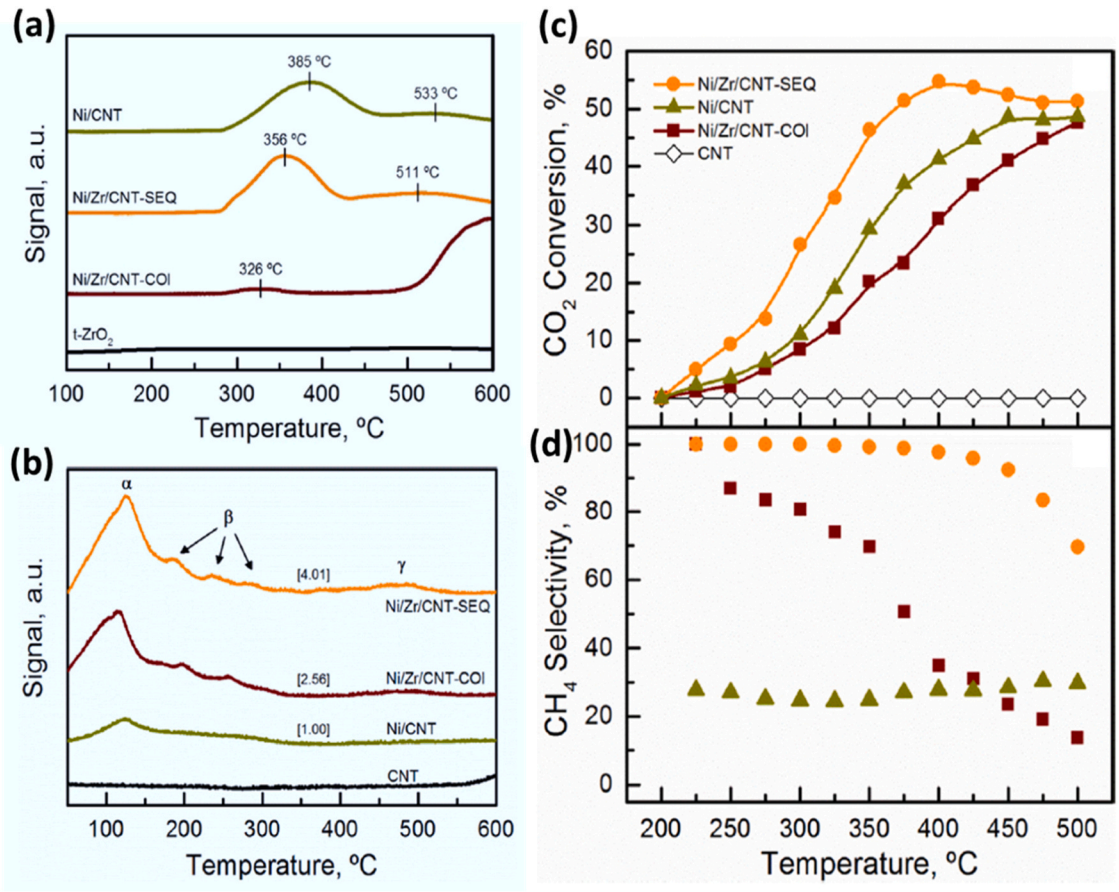


Fig. 3. (a) H_2-TPR profiles, (b) CO_2-TPD profiles, (c) CO_2 conversion, and (d) Selectivity to CH_4, of Ni/Zr/CNT-SEQ. Reproduced from [27] with permission of Elsevier.

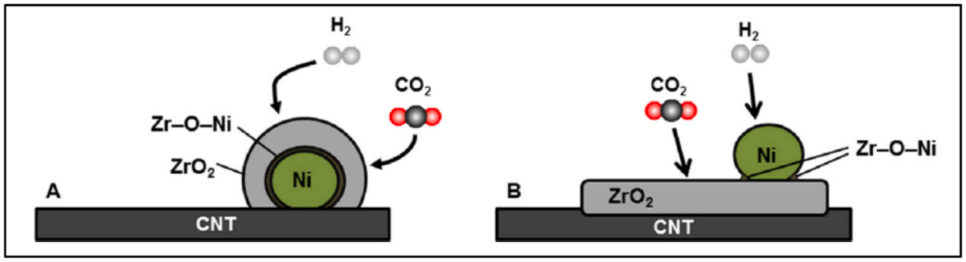
the reaction gases, which facilitate combination of hydrogen atoms with activated CO_2. On the other hand, the Ni/ZrO_2 interface in Ni/Zr/CNT-COI is not accessible to the reagents, which limits the dissociation of hydrogen and the rate of CO_2 methanation, as shown in Scheme 1.

Ni/N-doped CNT was synthesized via a three-step approach and studied as a catalyst for CO_2 methanation [28]. Firstly, a multiwalled carbon nanotube (MWCNT) was oxidized, using HNO_3. Then N-CNT was synthesized by annealing the oxidized CNT at 400 °C under ammonia. Ni/N-CNT was prepared by impregnation and calcination in air at 280 °C. The metal content was changed from 10 to 50 wt%. The optimum metal content was 30–40 wt% Ni, where it afforded the highest Ni surface area, the highest degree of CO_2 conversion, and the highest selectivity to methane (Table 2). The calculated apparent activation energy of different loadings ranged between 56 and 68 kJ mol^{-1}, while a constant TOF of 0.3 s^{-1} was recorded.

Dyachenko et al. studied the catalytic performance of $Co_{80}Ni_{20}$/

Table 2
CO_2 conversion, product selectivity, and TOF at 340 °C [28].

Catalyst	CO_2 Conversion (%)	CH_4 Selectivity (%)	CO Selectivity (%)	TOF (S^{-1})
10Ni/NCNT	28.5	81.4	18.5	0.30
20Ni/NCNT	35.4	90.4	9.5	0.28
30Ni/NCNT	50.9	95.8	4.2	0.28
40Ni/NCNT	51.4	95.6	4.4	0.32
50Ni/NCNT	46.9	93.7	6.3	0.32



Scheme 1. The NiO, ZrO_2 and interface Ni-O-Zr in the surface of CNT for Ni-Zr-CNT-COI (A) and Ni-Zr-CNT-SEQ catalysts (B). Reproduced from [27] with permission of Elsevier.

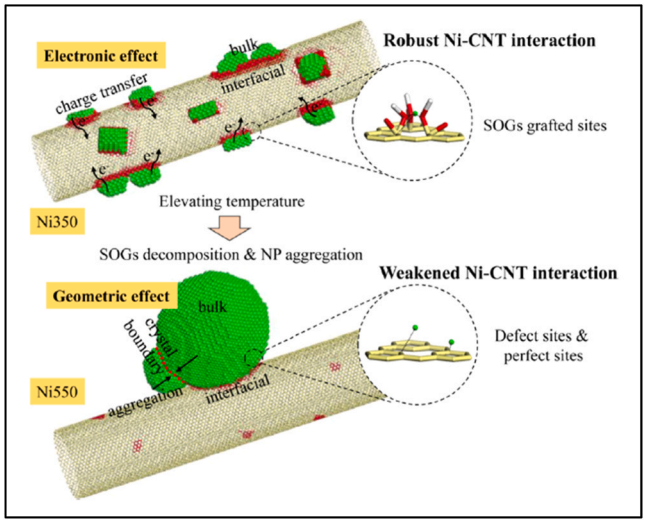
CNTs, $Ni_{80}Fe_{20}$/CNTs, and $Co_{93}Fe_{07}$/CNT towards CO_2 methanation [29]. The results showed that $Ni_{80}Fe_{20}$/CNTs afforded the highest CH_4 yield (88 %) at 350 °C, whereas $Co_{93}Fe_{07}$/CNT and $Co_{80}Ni_{20}$/CNTs provided CH_4 yield of 64 % and 72 %, respectively. In addition, N-doped CNT (CNT-N) was synthesized by ball milling of CNT with melamine and annealing the product under N_2 at 600 °C [30]. Afterwards, Ni/CNT-N was synthesized by incipient wetness impregnation and investigated as a catalyst for CO_2 methanation compared to Ni/CNT. No significant change was observed in the textural properties of pristine CNT and N-CNT. Ni/CNT-N afforded a maximum CO_2 conversion of 81.2 % and 99.2 % CH_4 selectivity at 400 °C, while the pristine Ni/CNT revealed a maximum CO_2 conversion of 78.5 % and 98.5 % methane selectivity at a higher temperature (430 °C). In addition, Ni/CNT-N exhibited excellent durability over 48 h time-on-stream.

Jing Li et al. investigated the catalytic activity of Mn-promoted Ni/oxygen functionalized CNT towards CO_2 methanation [31]. The as-synthesized catalyst was calcined under N_2 at three different temperatures; 350, 450 and 550 °C. In addition, the introduction of Mn into the structure made the Ni reduction more difficult, as it shifted the reduction temperature to higher temperatures. It was observed that elevating the calcination temperature increased the porosity of the CNTs and increased the particle size of Ni. However, the addition of Mn had no significant effect on the average particle size. The results also exhibited that the higher the calcination temperature, the weaker the metal support interaction (MSI)[31], which is opposite to the M-M_xO_y system. This was explained based on a mechanism emphasizing both the electronic and geometric effects (Scheme 2). Electrons are transferred from the Ni to CNT owing to the high electronegative electron-withdrawing nature of –COOH groups (electronic effect).

Furthermore, upon heating at temperatures > 400 °C, the surface oxygenated groups (SOGs) that anchor the Ni NPs, are decomposed [31]. These SOGs have higher binding force to Ni than the defect sites. Therefore, tiny Ni nanoparticles are agglomerated to large spherical NPs (geometric effect). The catalytic performance of Ni/CNT and Mn-promoted Ni/CNT catalysts revealed that CO_2 conversion, CH_4 selectivity, and CH_4 yield decreased with decreasing the calcination temperature (Fig. 4a–c). In addition, the presence of Mn remarkably enhanced the catalytic performance[31]. This was assigned that Mn facilitates the activation of reactants at low temperatures and increases the prevalence of Ni particles composed of several smaller domains, as well as introducing more defects in the Ni NPs.

The catalytic activity of Ni/N-doped CNT (Ni/CNT) was studied as a catalyst for CO_2 methanation [32]. N-CNT was first synthesized by chemical vapor deposition (CVD), using a $C_2H_6/NH_3/H_2$ mixture in a molar ratio of 2/2/1. Afterwards, Ni was deposited on N-CNT using incipient wetness impregnation. The CO_2 conversion increased with increasing the temperature to 200–360 °C, whereas the CH_4 selectivity was almost 99 % at the whole temperature range [32]. The calculated activation energy was found to be (38 kJ mol^{-1}). The impact of the gas hourly space velocity (GHSV) and CO_2: H_2 ratio were studied. The results showed that increasing the GHSV from 60,000 to 120, 000 mL min^{-1} led to a decrease in the CO_2 conversion from 80 % to 73 % with a slight decrease in CH_4 selectivity from 99 % to 94 % (Fig. 5a-b) [32]. Increasing the ratio of CO_2:H_2 from 4:1–6:1 increased the CO_2 conversion from 75 % to 92 % and the methane selectivity from 94 % to 98 % (Fig. 5c-d). The enhancement provided by N-doping is attributed to providing preferential binding sites for the stabilization of Ni NPs, generation of CO_2 concentration gradients at the catalyst active phase, and suppression of coke formation [32].

Briefly, the Ni catalyst, promoted by Ce and supported on multiwall carbon nanotubes (Ni-Ce/MWCNT) [28] showed an interesting performance, achieving the highest CH_4 selectivity (100 %) and 83.8 % of CO_2 conversion at 350 °C (Table 3). Besides, the Ni catalyst, promoted by Fe and supported on carbon nanotubes (Ni-Fe/CNTs) [29] presented 100 % carbon dioxide conversion and 88 % methane yield at 350 °C as well (Table 3). These two catalysts can be considered as the best reported catalysts for the CO_2 methanation, not only among the CNTs-supported catalysts, but also among the reported carbon-supported catalysts reported for the CO_2 methanation.



Scheme 2. The proposed mechanism accounting for the interaction between Ni and CNT. Reproduced from [31] with permission of ACS.

4. Graphene support

Graphene is characterized by several structural merits, such as high surface area, excellent thermal conductivity, high mechanical strength, environmental compatibility, low cost, and high adsorption capacity for a wide range of molecules [33,34]. The reduced oxide graphene (RGO) contains several functional groups, such as hydroxyls, epoxides, and carboxyl groups, which can act as centers for anchoring different types of catalyst nanoparticles [33]. This can significantly improve the dispersion of these nanoparticles on the support [34]. Ni/rGO was studied for CO_2 methanation by many authors, for example, graphene intercalated Ni-SiO_2/GO-Ni-foam was synthesized by deposition of graphene oxide (GO) on Ni-foam followed by the formation of nickel silicates [35]. Furthermore, the physicochemical properties of the catalyst were studied compared to Ni-SiO_2/Ni-foam, GO-Ni-foam, Ni-foam, and Ni-SiO_2 [36].

Ni-SiO_2/Ni-foam showed higher specific surface area and higher porosity than its counterparts [36]. The H_2-TPR revealed a stronger metal-support interaction on Ni-SiO_2/GO-Ni-foam compared to Ni-SiO_2/Ni-foam (Fig. 6a). The catalytic activity of the catalysts was investigated towards CO_2 methanation in the temperature range of 230–470 °C [36]. The results showed that the activity in terms of CO_2 conversion and methane yield follows the order: Ni-SiO_2/GO-Ni-foam > Ni-SiO_2/Ni-foam > Ni-SiO_2 > GO-Ni-foam ~ Ni-foam (Fig. 6b-c). DFT calculations showed that the addition of intercalating graphene decreased the reaction barriers and energies of H_2 and CO_2 dissociation, decreased the electronic density at the surface of nickel d band center, decreased the adsorption energy of H_2 and increased the CO_2 adsorption energy [36].

Nickel encapsulated in microporous graphene-like carbon (Ni@MGC) was synthesized via a multistep approach and studied for CO_2 methanation[37]. Firstly, furfuryl alcohol (FA) was impregnated into NaY zeolite and polymerized by heating at 150 °C to form PFA-NaY. Afterwards, the product was heated under N_2 then, under 2 % propylene/N_2 mixture to form carbon/NaY zeolite complex (NaY-C), which was treated with HF/HCl mixture to remove the NaY template and form MGC. Finally, Ni was deposited into MGC by incipient wetness impregnation [37]. The Ni loading was changed from 5 % to 20 %, where 15 % Ni@MGC afforded the best catalytic performance. It

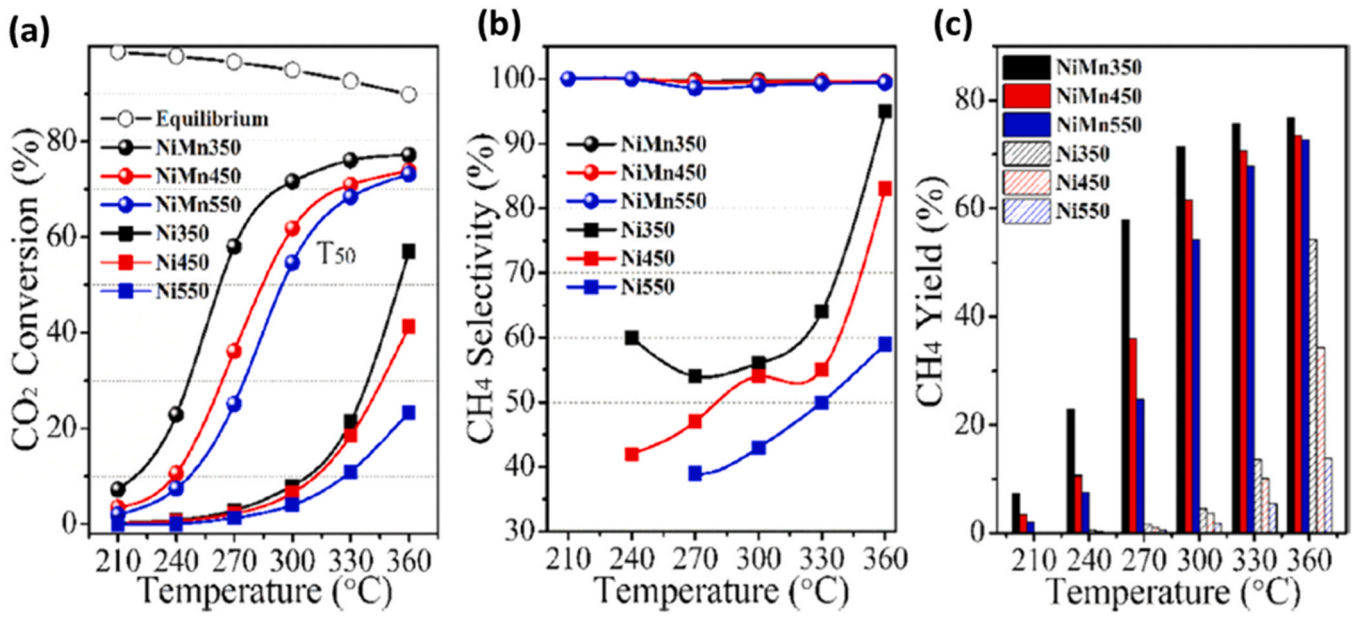


Fig. 4. CO_2 conversion (a), CH_4 selectivity (b), and CH_4 yield (c) for Ni and Mn-promoted Ni catalysts at atmospheric pressure, 100 mg catalysts, H_2/CO_2 molar ratio = 4:1. Reproduced from [31] with permission of ACS.

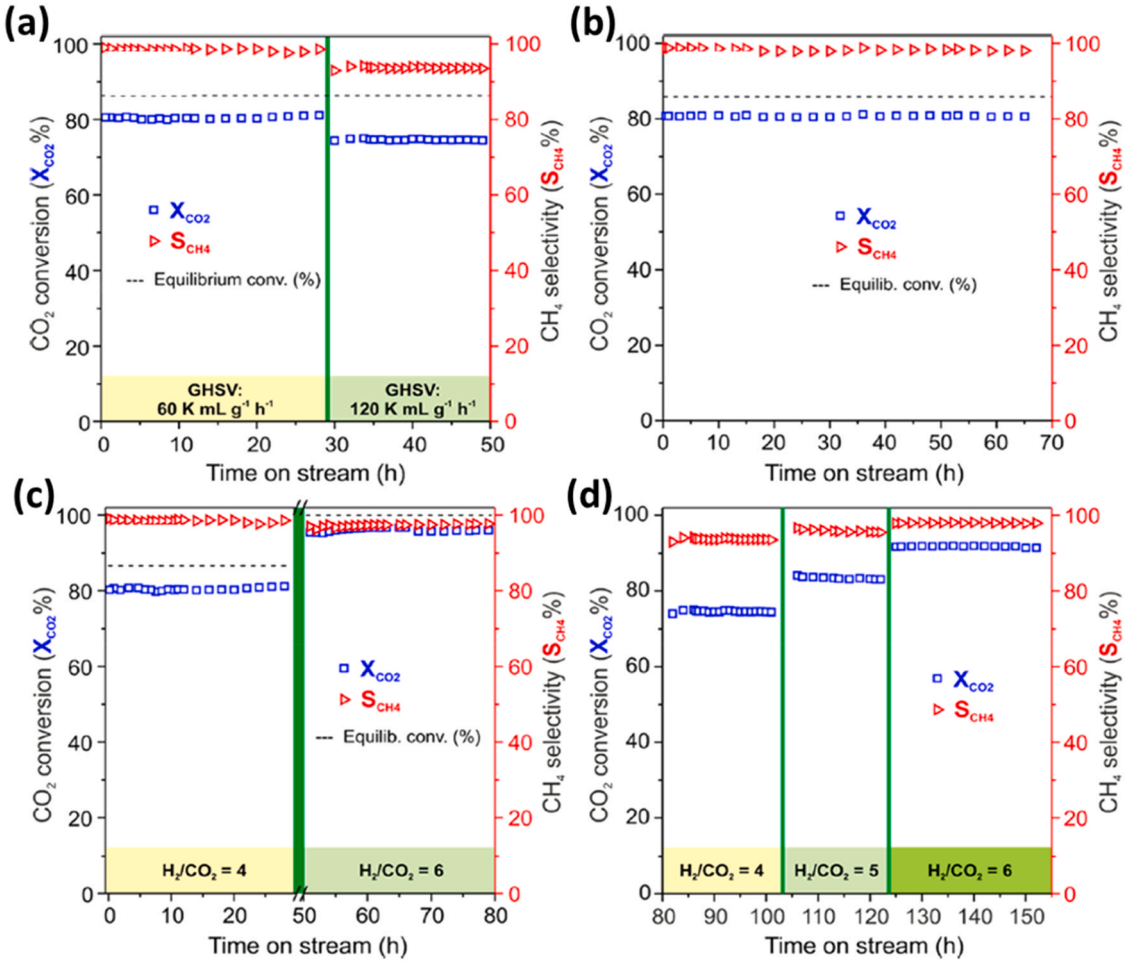


Fig. 5. (a) Effect of GHSV on the catalytic activity, (b) Long-term stability test at a GHSV of 60,000 mL g^{-1} h^{-1}, (c) Effect of H_2/CO_2 ratio on the catalytic performance at a GHSV of 60,000 mL g^{-1} h^{-1} and (d) Effect of H_2/CO_2 ratio on the catalytic activity at a GHSV of 120,000 mL g^{-1} h^{-1}. Reproduced from [32] with permission of ACS.

Table 3
A comparison among the catalytic activity of the reported CNT-based catalysts.

Catalyst	Promoter (wt%)	Metal Loading (wt%)	Preparation method	Optimal Temp. (°C)	GHSVmL/(g_{cat}.h)	Max. CO_2 Conv. (%)	Max. CH_4-S (%)	Max. CH_4-Y (%)	Ref.
5Co/CNTs	-	5	Wet Impregnation	300	2000	0	0	/	[25]
5Co/CNTs (activated)		5				14	25		
45Co/CNTs		45				89	100		
5Co/CNFs		5				26	80		
0.56Co/FLG		0.56				0	0		
5Co/FLG		5				22	37		
15Co/FLG		15				35	20		
15Co/CNTs–Al_2O_3		15				60	100		
25Co/CNTs–Al_2O_3		25				72	100		
12Ni4.5Ce/CNT			Ultrasonic-assisted impregnation	400	30,000	82.5	100	/	[26]
Ni/Zr/CNT-SEQ	-	5	Sequential impregnation	350	75,000	~ 54	95	~ 53	[27]
Ni/Zr/CNT-COI		5	Co-impregnation	350	75,000	~ 47	40	~ 13	[27]
Ni/MWCNT	-	12	Ultrasonic-assisted Co-impregnation	350	30,000	61.1	96.6		[28]
NiCe/MWCNT	Ce (4.5 %)	12				83.8 %	100		
$Co_{80}Ni_{20}$/CNTs $Ni_{80}Fe_{20}$/CNTs $Co_{93}Fe_{07}$/CNTs	-	20	Wet impregnation	350	50,000	100	-	72	[29]
				350		100		88	
				350		100		64	
Ni/N-CNT	-	10.7	Incipient impregnation	360	60,000	75	99		[30]
10Ni/NCNT	-	9.9	Wet impregnation	340	50,000	28.5	81.4		[30]
20Ni/NCNT		19.7				35.4	90.4		
30Ni/NCNT		28.9				50.9	95.8		
40Ni/NCNT		34.7				51.4	95.6		
50Ni/NCNT		46.0				46.9	93.7		
NiMn350/ CNT	Mn (4 %)	15	Ultrasonic co-impregnation	300	30,000	71.6	100	~ 71	[31]
Ni350/CNT		15				8.0	~ 56	~ 5	
Ni/N-CNT	-	15	Incipient impregnation	400	60,000	81.2	99.2		[32]
Ni/CNT				430		78.5	98.5		

provided a space-time yield of 2066 g_{CH4} kg_{cat}^{-1} h^{-1} at 400 °C, a turnover frequency (TOF) for CO_2 conversion is 7.4 × 10^{-2} s^{-1}, and apparent activation energy (E_a) of 75.32 kJ mol^{-1}. In addition, the same sample showed enhanced stability for 30 h time-on-stream at 400 °C compared to Ni/commercial carbon supports, owing to the isolation and confinement of Ni nanoparticles.

Feiyang Hu et al. investigated CO_2 methanation over NiCe supported on reduced graphene oxide (Ni-Ce/RGO) [38]. Compared to AC and γ-Al_2O_3-supported catalysts, Ni-Ce/RGO presented the highest catalytic activity with a maximum CO_2 conversion of 84.5 % at 350 °C, while Ni-Ce/AC and Ni-Ce/γ-Al_2O_3 exhibited a maximum conversion of 75.2 % at 350 °C and 78.7 % at 400 °C, respectively. In addition, the stability test for 100 h at 450 °C showed the following order of activity Ni-Ce/RGO > Ni-Ce/γ-Al_2O_3 > Ni/RGO > Ni/γ-Al_2O_3 > Ni-Ce/AC > Ni/AC [38]. The catalytic activity of Ni-Ce/RGO was confirmed by DFT calculations, which showed that Ce_2O_3 is much stronger interacting with RGO than Ce_2O_4. In addition, the adsorption of CO_2 is much stronger than H_2 on all catalysts. Furthermore, ceria remarkably promoted the activation of CO_2. In addition, CO_2 methanation was studied using Ni/rGO catalyst [39]. The Ni loading was varied between 10 and 20 wt %. Among the rGO-supported Ni catalysts, Ni15/rGO offered the highest specific surface area. Moreover, it exhibited the highest reduction temperature and the strongest basic sites compared to the other samples. The catalytic performance of different Ni/rGO samples was investigated towards CO_2 methanation in the three-phase slurry reactor at 240 °C and 10 bar [39]. Notably, Ni15/rGO showed the highest CO_2 conversion (55.3 %) and methane productivity of 24.9 g/kg_{cat} h compared to Ni10/rGO (44.3 %, 19.9 g/kg_{cat} h) and (40.5 %, 18.2 g/kg_{cat} h) for Ni10/rGO and Ni20/rGO, respectively. The superior catalytic performance of Ni15/rGO was assigned to the high surface area, strong basic sites, and enhanced MSI compared to its counterparts.

Ni/graphene aerogel (Ni/GA) was prepared by hydrothermal treatment of GO and nickel nitrate mixture in the presence of ammonia for cross-linking and investigated as a catalyst for CO_2 methanation compared to Ni/GO [40]. Ni/GA showed higher dispersion (0.095) with Ni particle distributions 5–15 nm compared to Ni/GO (0.065 and 5−30 nm). In addition, Ni/GA has enhanced reducibility, more adsorption active sites, and stronger MSI than Ni/GO. In-situ DRIFTS spectroscopy affirmed that formate is the main reaction intermediate. Ni/GA depicted higher CO_2 conversion (80.4 %) compared to Ni/GO (68.3 %) at 350 °C. Furthermore, higher methane yield was obtained over the Ni/GA (76.2 %) compared to Ni/GO (63.9 %).

Mohanty et al. studied the CO_2 methanation under induction heating mode (IH) using Ni-supported on a hybrid support, i.e., carbon nanofibers/few layer graphene (CNFs/FLG) [41]. The synthesis of the catalyst was carried out by the CVD at operating temperatures 700, 800 or 900 °C, and the Ni loading was changed; 10, 20, and 40 %. FC-800 showed the highest edge-to-surface, owing to the small diameter of CNF (18–23 nm) compared to FC-700 (33–45 nm) and FC-900 (85–95 nm) [41]. All samples revealed the presence of basic sites with moderate basicity with absence of weak basic sites, and FC-800 samples desorb at lower temperatures than FC-700 and FC-900 samples, which make them better candidates for CO_2 methanation. FC-800–10Ni exhibited the best catalytic performance with maximum CO_2 conversion of 85 % and 99.6 % methane selectivity at 360 °C. Increasing the H_2:CO_2 ratio from 4:1–6:1 increased the CO_2 conversion to 96.8 % and the CH_4 selectivity to 99.8 % (Fig. 6d). In addition, the increase of GHSV to 60, 000 and 120,000 decreased the maximum CO_2 conversion by 3 and 8 %, respectively, with little effect on CH_4 selectivity (Fig. 6e).

Effect of (d) feed mixture ratio and temperature and (e) GHSV on the CO_2 conversion and CH_4 selectivity for FC-800–10Ni. Reproduced from [41] with permission of Elsevier.

Graphene-supported Ni catalysts were studied and their catalytic behavior towards CO_2 methanation was compared to Ni supported alumina[42]. The studied graphene supports were commercial reduced graphene oxide (rGO), graphene oxide reduced with methylamine borane (BGO), aminated graphene oxide (AGO) and three types of oleylamine aminated graphene oxide prepared using different procedures (Ol/GO), (Ol-GO) and Ol-GO (Met). Among them only 13Ni/rGO catalyst retains functional oxygen groups in an accessible way. The

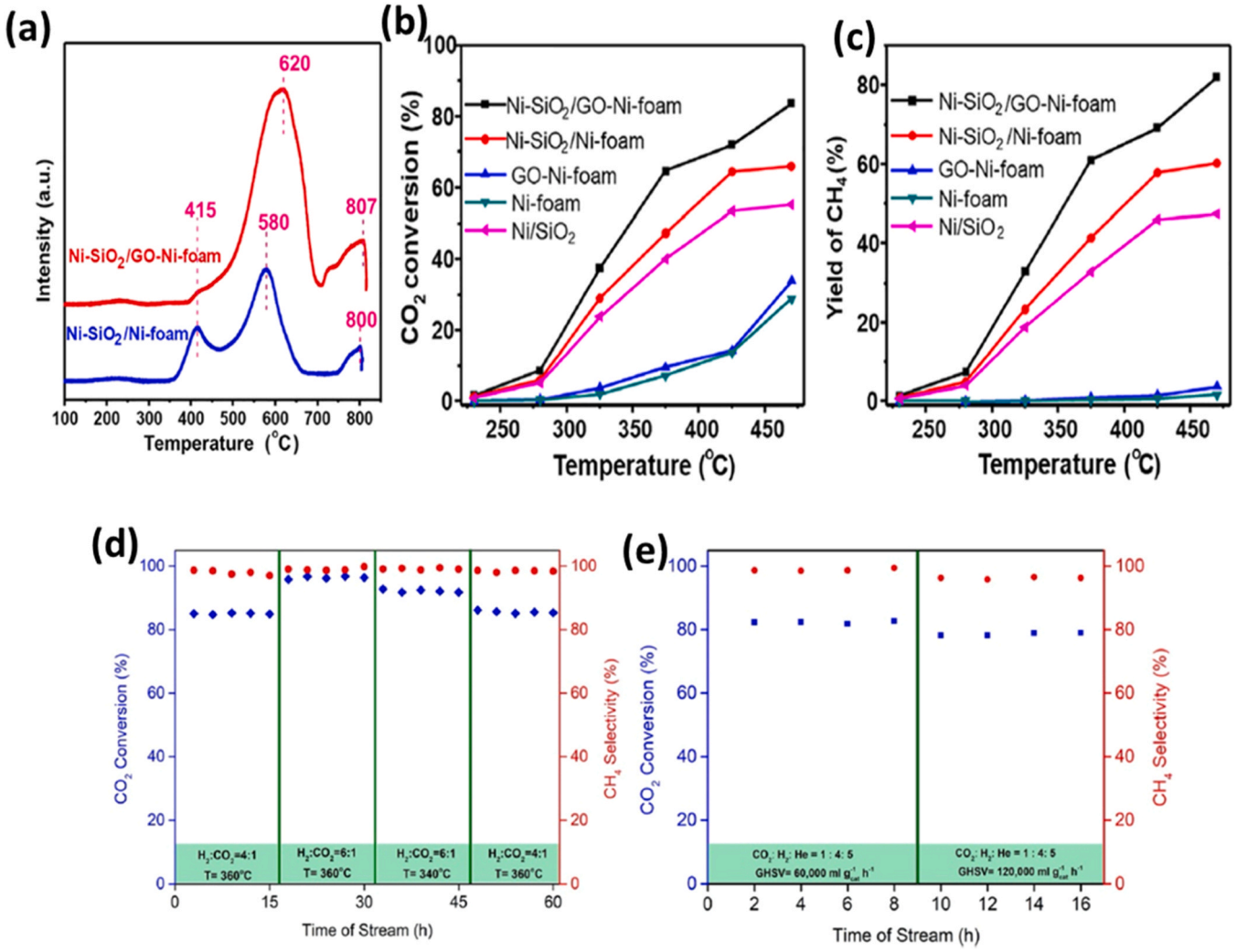


Fig. 6. (a) TPR profiles of Ni-SiO_2/GO-Ni-foam, Ni-SiO_2/Ni-foam catalysts, (b) CO_2 conversion and (c) CH_4 yield of different catalysts at 1.0 g cat., 0.1 MPa. GHSV = 500. Reproduced from [36] with permission of Elsevier.

introduction of lanthanum as promoter increased the catalyst resistance to H_2S poisoning and enhanced the catalytic activity of 13Ni/Al_2O_3 but did not affect the catalytic performance of 13Ni/rGO.

The impact of Ni particle size on the catalytic activity, stability, and methane selectivity was studied [43]. Ni nanoparticles of sizes ranging between 3.7 and 7.6 nm were deposited on graphene nanoplatelets (GNP-500) via the wetness impregnation method and studied for CO_2 methanation. The reaction was carried out at 1 and 30 bar. The measurements showed that at both pressures the increase in the Ni particle size increased the CO_2 conversion without affecting the apparent

Table 4
A comparison among the catalytic activity of the reported graphene-based catalysts.

Catalyst	Promoter	Metal Loading (wt %)	Preparation method	Optimal Temp. (°C)	GHSVmL/($g_{cat.}$ h)	Max CO_2 Conv. (%)	Max CH_4-S (%)	Max CH_4-Y (%)	Ref
Ni-SiO_2/GO-Ni-foam	-		Hydrothermal Synthesis	470	500	83.7	91	82	[36]
Ni-SiO_2/Ni-foam						66		~60	
Ni/SiO_2						55.2		47.4	
GO-Ni-foam						33.9		~ 3	
Ni-foam						28.9		~ 3	
Ni@MGC	-	15	Incipient impregnation	400	36,000	50	96		[37]
Ni-Ce/RGO	Ce (5 %)	20	Impregnation	350	36,000	84.5	99.9	83	[38]
Ni15/rGO	-	15	Incipient impregnation	240		55.3	100		[33]
Ni/GA	-		Hydrothermal Synthesis	350	36,000	80.4	94.8	76.2	[40]
Ni/GO						68.3	93.5	63.9	
FC−800–10Ni-F	-	10	Wetness impregnation	360	30,000	85	99.6		[41]
13Ni/rGO	-	13	Wetness impregnation	537	128.75	-	-	78	[42]

activation energy. In addition, the CH_4 selectivity is higher for larger particles at both 1 and 30 bar. Briefly, the Ce-promoted Ni catalyst, which is supported on reduced graphene oxide (Ni-Ce/RGO) [38] showed 83 % CO_2 conversion with 99.9 methane selectivity at 350 °C (Table 4), competing with the aforementioned catalysts Ni-Ce/MWCNT [28] and Ni-Ce/CNTs [29].

5. Biochar supports

According to Web of Science, only few research articles were reported on the biochar used in the thermal CO_2 methanation process, which might be attributed to the low thermal stability of biochar that may make problems during the reaction, such as oxidizing to CO_2 [21]. However, some researchers modified those materials and investigated their performance in the CO_2 methanation. In 2019, Wang et al. [9]. reported biochar-based catalysts obtained from the Pinus sylvestris powder, which was pyrolyzed at different temperatures; 500, 600, and 700 °C, a nitrogen environment for one hour. The powder was also doped with nitrogen by using urea precursor during the pyrolysis process and then cooled down to room temperature. The collected powder was then treated by nitric acid and then the mixture was filtered and the obtained wet powder was dried at 80 °C [9]. Finally, Ru was impregnated to the obtained support with metal loading around 35∼42 wt% by the wet impregnation method, and the catalysts were denoted according to their pyrolysis temperatures as, Ru/NABC-500, Ru/NABC-600, and Ru/NABC-700.

The three catalysts worked successfully in the CO_2 methanation reactions, and Ru/NABC-600 showed high CO_2 conversion of 93 % and CH_4 selectivity of 99 % at 380 °C and 10 bar [9]. In another study, Also Wnag et al. [44]. investigated the same biochar support pyrolyzed at 600 °C, but with Ni as an active metal instead of Ru. The catalysts were prepared by the impregnation method with metal loading of 15 wt% of Ni, and then another promoted catalyst was prepared using Ce as a promoter. The promoted Ni-Ce catalyst showed higher catalytic performance than the non-promoted catalyst in the CO_2 methanation, which is attributed to the ability of Ce to enhance the metal dispersion on the biochar support [44]. The promoted Ni-Ce catalyst could achieve 88 % carbon dioxide conversion and 92 % methane selectivity at 360 °C and 10 bar pressure [44]. Moreover, Stasi et al. [45]. reported a wheat straw derived biochar impregnated with Ni and Ce with metal loadings of 20 and 30 wt%, respectively. That catalyst (BCCeNi) showed 65 % carbon dioxide conversion and 95 % methane selectivity at 400 °C and 10 bar [45].

Those three studies [9,44,45] opened the door for utilizing biochar in thermal CO_2 methanation. However, using Ru as an active metal [9] and applying high-pressure conditions are disadvantages, as they increase the cost of the CO_2 methanation process and preclude the possibility of scaling it up. Li et al. investigated the effect of Mg on the Ni/biochar-based catalysts, which were derived from coconut shells [46]. The coconut shell biochar showed high surface area and various pore sizes, which enhanced the catalytic activity [46]. Moreover, the addition of Mg improved the metal dispersion on the support resulting in high catalytic performance [46]. The catalytic tests that were carried out at atmospheric pressure showed that the catalyst, Ni-Mg/coconut shell biochar, was highly active in the CO_2 methanation, as it could achieve CO_2 conversion of 90 % and CH_4 selectivity of 99 at 450 °C [46]. This study presented a cheaper route for preparing biochar-based catalysts and affordable operating conditions in the CO_2 methanation process. However, the high catalytic performance was obtained at a higher operating temperature (450 °C) compared to the previous study carried out at 10 bar (360 °C) [44]. In addition, Renda et al. investigated the wheat straw biochar as a support for Ni in the CO_2 methanation reaction, which provided very high surface area leading to high catalytic activity (600 m^2/g) [45,47]. The authors also reported that addition of CeO_2 as a promoter to the nickel/ wheat straw biochar enhance the metal support interaction and improves the metal dispersion, leading to reduced active phase mobility and sintering resistance [47]. The best-promoted Ni-Ce/biochar catalyst could achieve 62 % carbon dioxide conversion and 90 % methane selectivity at 425 °C and atmospheric pressure [47]. In a further study, the same authors reported that the addition of 30 and 20 wt% of ceria and nickel, respectively resulted in higher catalytic activity as the catalyst 20Ni-30Ce/biochar achieved 65 % carbon dioxide conversion and 95 % methane selectivity at 400 °C [45].

Tarifa et al. [48] investigated cellulose-derived carbon (CDC) as a biochar support for the nickel in the CO_2 methanation. The CDC exhibited unique features, such as a significant surface area, high thermal conductivity, hydrophobic tendencies, and outstanding hydrogen storage capability [48]. These attributes prove highly beneficial in CO_2 methanation by promoting the efficient dispersion of the active metal, preventing the formation of hot spots, and providing hydrogen to the active phase. The catalyst that was promoted by Ce (Ni-Ce/CDC) showed a very high selectivity to methane (∼100 %) at very low operating temperature (175 °C) in addition to 54 % CO_2 conversion at the same temperature [48]. That high catalytic activity and selectivity is attributed mainly to the aforementioned catalytic properties of CDC and then to the Ce effect, improving the metal dispersion. Filipe et al. reported Cork derived carbon as supports for the catalysts of CO_2 methanation, which offered high affinity towards the methanation reactions [49].

Those carbonaceous materials showed high metal support interaction and high metal dispersion, leading to high catalytic activity, particularly after addition of Ce to the Ni [49]. The highest catalytic performance was offered by NiCe/biochar-Cork at 400 °C, showing 70 % carbon dioxide conversion and 99 % methane selectivity [49].

Recently, Gamal et al. reported sugarcane bagasse biochar (SCBB) as a support for the Ni to be used for the first time in the CO_2 methanation [50]. The SCBB-based catalysts, were synthesized by pyrolysis at 500 °C in the presence of Ni precursor. The catalysts were loaded by different Ni-nitrates concentrations; 0.1, 0.3, 0.5, 0.8 and 1.2 mmol/g, and accordingly, denoted as, 0.1Ni/SCBB, 0.3Ni/SCBB, 0.5Ni/SCBB, 0.8Ni/SCBB and 1.2Ni/SCBB, respectively [50]. The SCBB support offered high surface area (620 m^2/g) with porous structures, resulting in high catalytic activity, as shown in Fig. 7a-d. The zoom on the porosity showed the fishing net structures of the SCBB reported, earlier in the literature [51], as seen in Fig. 7e-f. Moreover, increasing the Ni loading on the SCBB more than 0.5 $mmol_{Ni}/g_{SCBB}$ led to agglomeration as depicted in Fig. 7g-h, which resulted in less catalytic activity [50]. The catalytic performance was increasing with raising the nickel content up to 0.5 mmol/g, then it dropped with increasing the nickel loading, ascribed to the agglomeration [50]. The catalyst 0.5Ni/SCBB exhibited the highest CO_2 conversion at 58 % (at 500 °C), CH_4 selectivity at 76 % (at 400 °C), and CH_4 yield at 34 % (at 400 °C), respectively (Fig. 8a-d). CH_4 selectivity and CH_4 yield followed the same trend, as they increased by raising the temperature to 400 °C, and then dropped because of the competed reverse water gas shift reaction [14,52].

Table 5 shows a comparison among the highest catalytic performance of the few biochar-based catalysts reported for the CO_2 methanation. All catalysts tested at high operating pressure (10 bar) could achieve high catalytic performance at 400 °C [9,44,45]. However, using high-pressure conditions results in higher costs. Thus, it is worth noting that four studies could achieve high catalytic performance at atmospheric pressure [47–50]. Among those four studies, the bimetallic catalyst Ni-Ce/CDC can be considered the best catalyst among all biochar-based catalysts reported for the CO_2 methanation, as it could achieve 78 % carbon dioxide conversion and 99.9 % methane selectivity at atmospheric pressure, at an operating temperature 400 °C. The catalyst Ru/ABC also achieved 99 % methane selectivity at 400 C, but using the expensive Ru and applying high pressure (10 bar) are significant disadvantages precluding the scaling up.

6. Activated carbon (AC)

Only three articles reported on the activated carbon (AC) as a support

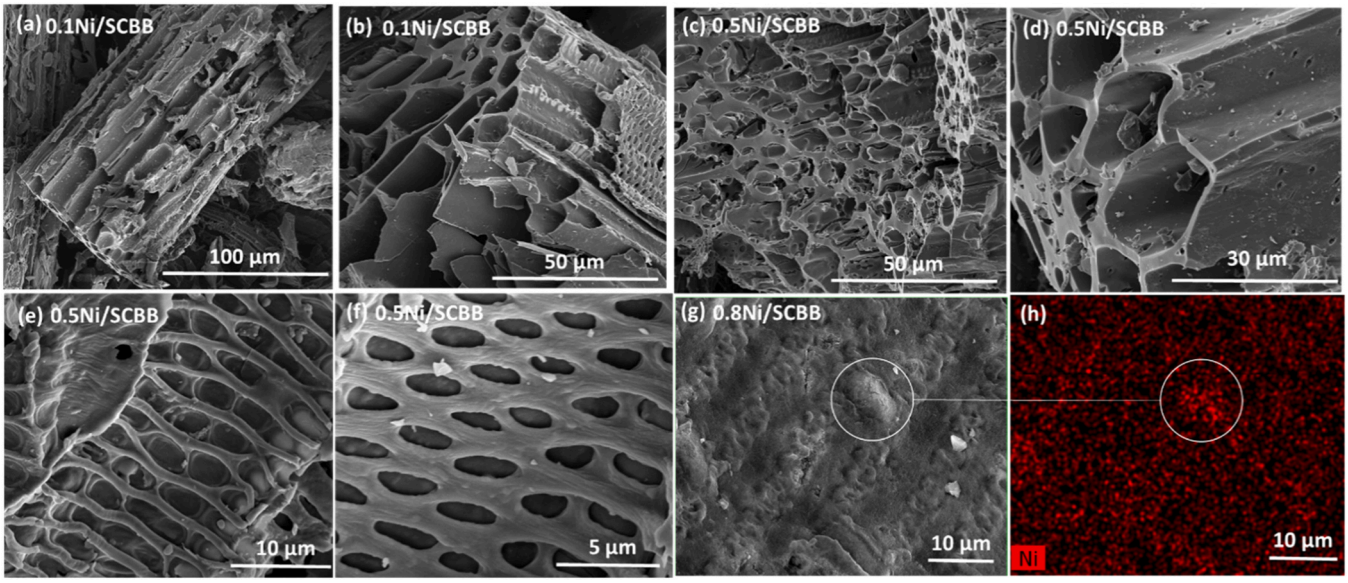


Fig. 7. (a–g) SEM images of different catalysts, and (h) nickel elemental mapping of 0.8Ni/SCBB. Reproduced from [50] with permission of Elsevier.

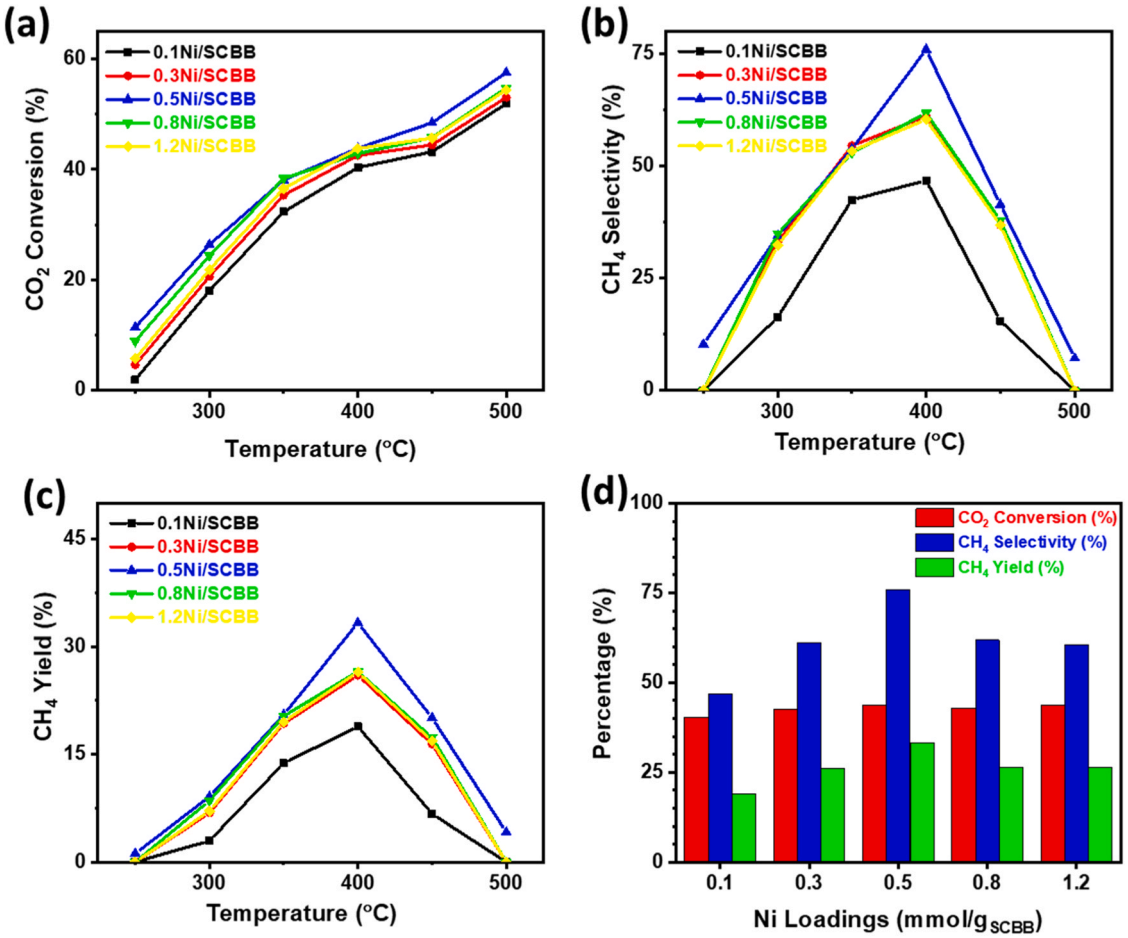


Fig. 8. (a) CO_2 conversion, (b) CH_4 selectivity, CH_4 yield of all Ni/SCB catalysts. Reproduced from [50] with permission of Elsevier.

for the catalysts used in the CO_2 methanation and all of them studied AC with Ni. Those articles indicated that the AC could provide high surface area and enhance the dispersion of the metal particles on the support [53–55]. Feng et al. reported that using AC as a support for Ni offered a very high surface area (940 m^2/g) and a pore volume of 0.51 cm^3/g, resulting in high catalytic performance [53]. The catalyst Ni/AC containing 15 wt% of Ni and prepared by impregnation method could achieve the highest catalytic activity at 360 °C with 68 % CO_2 conversion and 65 % CH_4 yield [53]. Goncalves et al. also reported 15 wt% Ni on activated carbon for the CO_2 methanation, prepared by incipient

Table 5
A comparison among the highest catalytic performance of the few reported biochar catalysts.

Catalyst	Metal Loading (wt%)	Operating Pressure	Optimum Temp. (°C)	GHSV mL/(g_{cat}.h)	Max. CO_2 conversion (%)	Max. CH_4 selectivity (%)	Ref.
Ru/ABC	35–42	10 bar	400	6000	90	99	[9]
Ni/ABC	15	10 bar	400	1200	85	91	[44]
Ni/Ce-ABC	20–30	10 bar	400	1200	88.6	91.5	[44]
Ni-Ce/BC	20–30	10 bar	400	15,000	65	95	[45]
Ni-Ce/BC	15–20	Atmospheric	450	6000	65	88	[47]
Ni-Ce/CDC	3.5–3.5	Atmospheric	400	30,000	78	99.9	[48]
NiCe/DC	15–15	Atmospheric	400	86,100	70	99	[49]
Ni/SCBB	15	Atmospheric	400	48,000	44	76	[50]

ABC= activated biochar carbon, BC= biochar carbon, CDC: cellulose-derived carbon, DC= derived cork, SCBB= sugarcane bagasse biochar.

wetness impregnation [54]. The catalyst Ni/AC achieved the highest catalytic activity at 425 °C with 72 % CO_2 conversion and 95 % CH_4 selectivity [54]. Wang et al. [55]. studied Ni catalysts supported on AC and synthesized by the incipient wetness impregnation with 10 wt% of Ni. The catalyst sowed 69 % CO_2 conversion and 96 % CH_4 selectivity at 340 °C [55].

7. Carbon nanofibers (CNFs)

Only two articles were reported on the carbon nanofibers (CNFs) as supports for the catalysts of the CO_2 methanation, indicating that CNFs can provide high surface area [56,57]. Jiménez et al. investigated three morphological types of carbon nanofibers as supports for Ru; platelet, fishbone, and ribbon. The catalysts were prepared by the Chemical vapor deposition (CVD) method with 0.5 wt% of Ru, and the authors claimed that the catalytic activity of the catalysts of CO_2 methanation is not affected by the nature of the CNFs supports [56]. However, the BET surface area analysis showed that the platelet type offered 286 m^2/g, while the fishbone and ribbon types presented 202 and 68 m^2/g, respectively [56]. The three Ru catalysts supported on the three types of CNFs showed similar catalytic activity with 52 % CO_2 conversion and 99 % CH_4 selectivity at 500 °C [56]. In addition, Gaidai et al. [57] investigated the effect of CNFs as a support for Fe-Co catalyst in the CO_2 methanation. Using the CNF as a support enhanced the catalytic activity, as Fe-Co alone presented 71 % CO_2 conversion and only 8 % CH_4 selectivity at 450 °C, while the supported catalyst (Fe-Co/CNFs) offered 65 % CO_2 conversion and 88 % CH_4 selectivity at 390 °C [57]. Hence, more work on the activated carbon and carbon fibers, as supports for the catalysts of CO_2 methanation are needed to explore their effect on the catalytic performance, which may improve it due to the offered high surface area of the activated carbon [53] and the high electrical conductivity of the carbon nanofibers [58].

8. Effect of promoters on the carbon-supported catalysts

Various promoters were reported for the carbon-supported catalysts used for the CO_2 methanation, such as Ce, Ca, Mg, and La. Most of the reported promoters were investigated with Ni as the active metal, and Ce was the most reported promoter for the carbon-supported Ni catalysts. Firstly, in 2016, Feng et al. [53]. investigated the effect of Ca, as a promoter on the catalytic activity of Ni catalyst supported on activated carbon with constant Ni loading 15 wt%. The catalysts were prepared by the impregnation method with different Ca contents; 0, 5, 10, 15, 20 wt %, and denoted as, 15Ni/AC, 15Ni5Ca/AC, 15Ni10Ca/AC, 15Ni15Ca/AC, and 15Ni20Ca/AC, respectively. The CO_2-TPD showed that 15Ni10Ca/AC has the highest CO_2 adsorption-desorption peak, which can correspond to the basicity of the catalyst and indicates that it has the most available active sites, which accordingly enhances the catalytic performance [53]. The catalytic tests at 360 °C showed that the catalytic activity increases with raising the Ca amount to 10 wt%, as Ca significantly affects the interaction between the Ni and the support [53]. Although the 15Ni/AC catalyst showed a CO_2 conversion of 35.89 % and a CH_4 yield of 24.2 %, 15Ni10Ca/AC presented 76.2 % CO_2 conversion and 75.5 % CH_4 yield. Increasing the Ca loading up to 20 wt% affected negatively the catalytic activity, which is attributed to the coverage of active sites [53].

Li et al. [46] tested the effect of Mg as a promoter on the Ni/coconut shell carbon catalysts that were synthesized by the co-impregnation method with a mass ratio of Ni to Mg 0.13, 0.26, 0.39, and denoted as Ni/CSC, Ni-Mg0.13/CSC, Ni-Mg0.26/CSC, Ni-Mg0.39/CSC. The addition of Mg enhanced the dispersion of Ni and accordingly prevented agglomeration of Ni particles at high temperatures, which was confirmed by the SEM [46]. In addition, the introduction of Mg improved the basicity of the catalysts, as indicated by the CO_2-TPD analysis [46]. By analyzing the area under the curves, which represents the basicity of the respective catalysts, it was concluded that Ni-Mg0.26/CSC demonstrates the highest level of basicity, leading to the highest catalytic activity. All promoted catalysts showed higher catalytic activity than the non-promoted catalyst. At 450 °C and atmospheric pressure, Ni-Mg0.26/CSC showed CO_2 conversion of 90.10 %, while Ni/CSC showed only 77.06 % with methane selectivity around 99 % for both catalysts. Ni-Mg0.39/CSC presented less catalytic activity than Ni-Mg0.26/CSC, which is attributed to the active site occupation caused by the excessive metal particles [46]. In addition, Mn is studied as a promoter for Ni nanoparticles (NPs) supported on carbon nanotubes (CNTs) [31].

The catalysts were synthesized by the ultrasonic co-impregnation method with fixed Ni and Mn loadings, 15 and 4 wt%, respectively in addition to another catalyst with only Ni loading. The addition of Mn significantly boosted the catalytic activity at low temperatures, which is attributed to the improved adsorption of CO_2, as indicated by the CO_2-TPD analysis [31]. However, this study was ambiguous, as it did not investigate different Mn loadings. Moreover, in a comparative study, Jurca et al. [59]. studied the effect of three promoters (Pd, Ca, and S) on Co-Fe catalysts supported on carbon (Co-Fe@C). It is concluded that the addition of Pd with small amounts around 0.5 wt% can improve the CO_2 conversion and CH_4 selectivity, which is attributed to enhancing the H_2 activation and spillover, caused by Pd [59]. In addition, incorporation of Ca with high percentage around 25 wt% can enhance both CO_2 conversion and CH_4 selectivity, which is ascribed to improving the CO_2 adsorption near to the active sites [59]. On the other hand, addition of small amounts of S to the catalysts showed a severe negative effect on the CO_2 conversion in addition to directing the selectivity to CO instead of CH_4 [59]. That dramatic effect is attributed to the poisoning of hydrogenating sites, caused by S, disfavoring not only the attack on CO_2 but also the successive hydrogen uptake toward CH_4 [59].

Regarding the Ce, which is the most reported promoter for the carbon-supported catalysts used in the CO_2 methanation, Hu et al. studied the effect of Ce on Ni-based catalysts supported on reduced graphene oxide (RGO) [38]. The catalysts were prepared by the impregnation method with 20 wt% of Ni and 5 wt% of Ce, and denoted as Ni/RGO and Ni-Ce/RGO. The catalytic performance were significantly increased after ceria addition. The Ni-Ce/RGO presented higher CO_2 conversion (84.5 %) and higher methane yield (83.0 %) at 350 °C

and atmospheric pressure, while Ni/RGO showed 78 % CO_2 conversion and 75 % CH_4 yield [38]. This high catalytic activity is ascribed to the support and promoter effects. RGO support provides high surface area and surface oxygen-containing functional groups, leading to stable anchoring of metals, and Ce improves the metal dispersion on the RGO in addition to enhancing the reaction because of the oxygen vacancies of Ce [38]. Besides, Renda et al. [47]. also studied the effect of Ceria on the catalytic activity of Ni/biochar (wheat straw) catalysts that were prepared by slow pyrolysis and subsequent activation with CO_2. All catalysts included 10 wt% of Ni with different CeO_2 contents as a promoter; 0, 10, 30 and 50 wt%, and denoted as BCNi, BCNiCe10, BCNiCe30, BCNiCe50, respectively. Introducing ceria to the Ni supported biochar catalysts up to 30 wt% provided higher surface area and enhanced the metal dispersion on the biochar support [47]. However, higher loadings of CeO_2 resulted in a decrease in the surface area. The catalytic activity tests were carried out at the range of 200–450 °C and showed that all CeO_2-promoted catalysts presented higher values of CO_2 conversion and CH_4 selectivity, compared to the BCNi catalysts. In addition, BCNiCe30 presented the highest catalytic activity with 70 % CO_2 conversion and 90 % CH_4 selectivity at 450 °C, which is attributed to the CeO_2 effect that increased the surface area and enhanced the metal dispersion on the support [47]. BCNiCe50 catalyst showed 50 % CO_2 conversion and 80 % CH_4 selectivity at 450 °C, which is attributed to the agglomeration occurred by the excess ceria, as confirmed by the TEM images [47].

In another comparison, Ahmad et al. [60]. investigated Ce compared to La as promoters for Ni-based catalysts supported on graphitic carbon nitride (g-C_3N_4). The catalysts were prepared by the impregnation method and the Ni amount was fixed at 10 wt%, and the promoter loading (Ce or La) was fixed at 3 wt%. The catalysts were denoted as Ni/g-C_3N_4, Ni-Ce/g-C_3N_4, and Ni-La/g-C_3N_4. Both Ce and La improved the metal dispersion leading to less agglomeration, and both of them enhanced the metal-support interaction [60]. The CO_2-TPD analyses showed that the basicity of catalysts followed the order of Ni-Ce/g-C_3N_4 > Ni-La/g-C_3N_4 > Ni/g-C_3N_4, indicating that Ce promoted the highest CO_2 adsorption, and accordingly the highest catalytic activity [60]. The catalytic activity tests were carried out in a temperature range of 225–600 °C, and Ni-Ce/g-C_3N_4 presented the highest catalytic activity among the three catalysts with 82 % CO_2 conversion and 99 % CH_4 selectivity at 300 °C. Ni-La/g-C_3N_4 and Ni/g-C_3N_4 showed the maximum CO_2 conversion of 73 % and 48 % at 342 and 425 °C, respectively, in addition to 99 % CH_4 selectivity during the whole range of temperatures 250–300 °C [60]. That high performance is attributed to the well-enhanced metal dispersion, improved surface basicity, and generation of surface oxygen vacancies, which originates from the reduction of CeO_2 and Ni-Ce-O mixed oxide [60]. However, La addition could also decrease the Ni particle size, enhancing the dispersion, which results in improving the catalytic activity due to the synergetic effect [42,60].

Tarifa et al. [48] reported a comparison between Ce and Mg as promoters for Ni-based catalysts supported on cellulose-derived carbon (CDC), synthesized by wetness impregnation with aqueous solutions of nickel, cerium, and magnesium nitrates. Nickel concentration was fixed at 3.5 wt%, and Mg and Ce were impregnated with atomic ratios of Ni: Mg = 1:1, Ni:Ce = 1:1, Ni/Mg/Ce = 1:0.5:0.5, followed by reduction for three hours at 600 °C in H_2. The collected catalysts were denoted as Ni/CDC, Ni-Mg/CDC, Ni-Ce/CDC, and Ni-Mg-Ce/CDC [48]. According to the average particle sizes calculated by the Scherrer equation, Ni/CDC showed the highest Ni particle size (27 nm), while Ni-Mg-Ce/CDC showed the smallest Ni particle size (8 nm). Ni-Mg/CDC catalysts

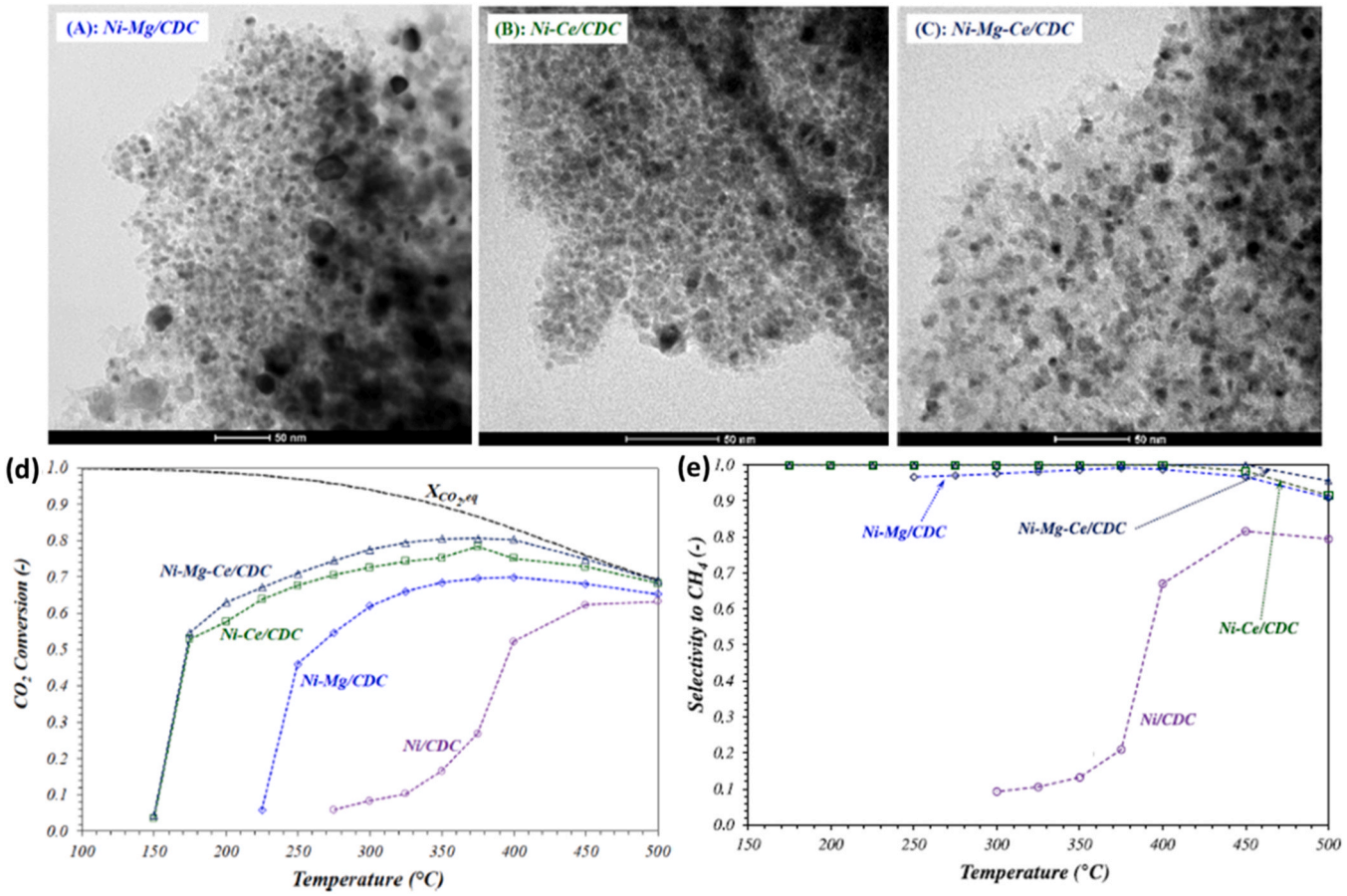


Fig. 9. TEM images of (a) Ni-Mg/CDC, (b) Ni-Ce/CDC, and (c) Ni-Mg-Ce/CDC. (d) CO_2 conversion and (e) CH_4 selectivity of all catalysts. Reproduced from [48] with permission of ACS.

displayed higher Ni particle size (21 nm) than Ni-Ce/CDC (10 nm), which is ascribed to the ceria with vacancies of oxygen that interact with Ni nanoparticles blocking its sintering [38,61]. The H_2-TPR profiles of the catalysts showed that Ni-Ce/CDC poses higher reducibility than Ni-Mg/CDC, which might be attributed to the highly dispersed and low-sized Ni nanoparticles caused by ceria addition [62]. In addition, the TEM images showed that Ni-Ce/CDC has better metal distribution than Ni-Mg/CDC, which is attributed to the well-known capacity of cerium to block sintering [61]. In addition, Ni-Mg-Ce/CDC showed the best metal distribution in addition to the smallest particle sizes as shown in Fig. 9a–c.

In the catalytic tests performed at a temperature range of 150–500 °C, Ni-Ce/CDC was superior to Ni-Mg/CDC at all temperatures, and the catalytic activities followed the trend; Ni-Mg-Ce/CDC > Ni-Ce/CDC > Ni-Mg/CDC > Ni/CDC, as shown in Fig. 9d. In addition, Ni-Mg-Ce/CDC and Ni-Ce/CDC were active at 150 °C, while Ni-Mg/CDC and Ni/CDC started to be active at 225 °C and 275 °C, respectively, as seen in Fig. 9d. At 375 °C as an optimal temperature, Ni-Ce-Mg/CDC and Ni-Ce/CDC showed the highest performance with ~80 % CO_2 conversion and ~100 % CH_4 selectivity, while Ni-Mg/CDC showed ~70 % CO_2 conversion and ~99 % CH_4 selectivity, and finally the non-promoted Ni/CDC showed the worst CO_2 conversion and CH_4 selectivity among all catalysts, as shown in Fig. 9d-e. Hence, the effect of Ce on the Ni catalysts supported on cellulose-derived carbon is better than the Mg effect on the same catalysts due to offering smaller particle sizes with higher reducibility [48]. Kim et al. [63]. reported similar results for the effect of Ce and Mg on Ni catalysts supported on low-rank coal with constant Ni loading of 15 wt% and Ce or Mg loading of 3 wt%. The authors attributed the higher effect of Ce to improving the high surface area and enhancing the reducibility of Ni [63].

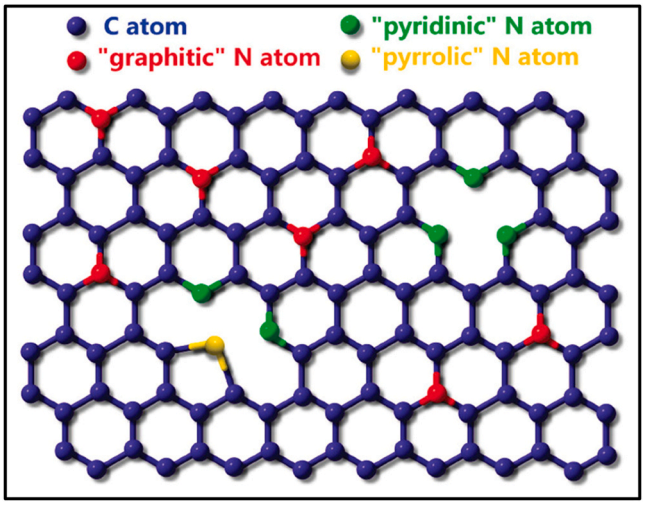
Table 6 shows a comparison among the most promising promoted carbon-supported catalysts reported for CO_2 methanation, which can indicate that Ce is the most common and effective promoter used in CO_2 methanation. In addition, other promoters were reported for the carbon-supported catalysts, such as Ca, Mg, and La, as shown in Table 6. The highest catalytic performance was reported on the catalyst Ni-promoted Ce with a loading of 4.5 wt% Ce, which achieved 83.8 % CO_2 conversion and 100 % CH_4 selectivity at 350 °C only [28]. The La-promoted catalyst presented less catalytic activity than Ni-Ce/MWCNTs, but higher than the Mg-promoted catalyst. The Ni-Mg/CDC with Mg loading of 3.5 wt% achieved 70 % CO_2 conversion and 99 % CH_4 selectivity at 375 °C [48]. Besides, Ca was reported as a promoter presenting high catalytic activity, a Ni-Ca/AC with 10 wt% Ca loading achieved 76.22 % CO_2 conversion and 75.53 % CH_4 yield at 360 °C [53].

9. Effect of N-doping on the carbon-supported catalysts

It is reported that N-doping into the carbonaceous materials used in the CO_2 methanation is crucial for enhancing the catalyst stability, and metal dispersion, and improving the support basicity, resulting in higher catalytic performance [28,30]. In addition, Roldan et al. [64]. reported that nitrogen doping into the carbonaceous materials for CO_2 methanation can enhance intensively the CO_2 adsorption and accordingly improve the CO_2 conversion rates [64]. N-doping requires the substitution of carbon atoms in the skeleton for nitrogen atoms, which causes charge redistribution, resulting in the modification of catalytic properties [65,66]. Using XPS for different N-doped graphene samples, Wei et al. reported that the blank graphene did not N1s peak, as expected, while the N-doped samples showed N1s peak with three components, concluding that nitrogen atoms were represented in the three different bonding characters, doped into the graphene network as graphitic, pyridinic, and pyrrolic, creating the defects, as shown in Scheme 3[67].

Wang et al. investigated the nitrogen-doped biochar as support for Ru in the CO_2 methanation, reporting that the pyrolysis temperature of the biochar support has a clear impact on the nitrogen species proportions in the biochar [9]. The authors carried out the pyrolysis using urea as a nitrogen source and $NaHCO_3$ as an activator. The pyrolysis temperature variations resulted in different nitrogen species (pyridinic-N, pyrrolic-N, and graphitic-N), as shown in Fig. 10[9]. N-doped activated biochar, pyrolyzed at 600 °C, and denoted as N-ABC-600 included the highest pyridinic-N content (37.7 %), followed by N-doped activated biochar, pyrolized at 500 C, which denoted as N-ABC-500 (31.4 %) and then N-doped activated biochar, pyrolized at 700 C, which denoted N-ABC-700 (26.6 %) [9]. The authors claimed that N-ABC-600 demonstrated the highest catalytic performance with the highest CO_2 conversion, which is attributed to the higher pyridinic-N content [9].

Ly et al[68]. reported that the nitrogen doping into the carbonaceous supports of the CO_2 methanation can also enhance the reducibility. The authors investigated nitrogen-doped carbon nanotubes for Fe with metal loading of 31.2, 33.5, and 38.3 wt%. The catalysts were synthesized



Scheme 3. Schematic representation of the N-doped graphene. Reproduced from [67] with the permission of ACS.

Table 6
A comparison among the most promising promoted carbon-supported catalysts reported for the CO_2 methanation.

Catalyst	Promoter	Metal Loading (wt%)	Preparation method	Optimal Temp. (°C)	Max. CO_2 Conv. (%)	Max. CH_4-S (%)	Max.CH_4-Y (%)	Ref
Ni-Ce/RGO	Ce	20–5	Wet Impregnation	350	84.5	/	83	[38]
BCNiCe30	Ce	10–30	activation with CO_2	450	70	90	/	[47]
BCNiCe50	Ce	10–50	activation with CO_2	450	50	80	/	[47]
Ni-Ce/CDC	Ce	3.5–3.5	Wetness impregnation	375	80	100	/	[48]
Ni-Mg-Ce/CDC	Mg-Ce	3.5–1.75–1.75	Wetness impregnation	375	80	100	/	[48]
Ni-Ce/MWCNT	Ce	12–4.5	Ultrasonic impregnation	350	83.8 %	100	/	[28]
Ni-Mg/CSC	Mg	10–2.6	Co-Impregnation	450	90.1	99	/	[46]
Ni-Mg/CDC	Mg	3.5–3.5	Wetness impregnation	375	70	99	/	[48]
NiCa/AC	Ca	15–10	Impregnation method	360	76.22	/	75.53	[53]

AC; activated carbon, CSC: coconut shell carbon, RGO: reduced graphene oxide, BC: biochar, CDC: cellulose-derived carbon.

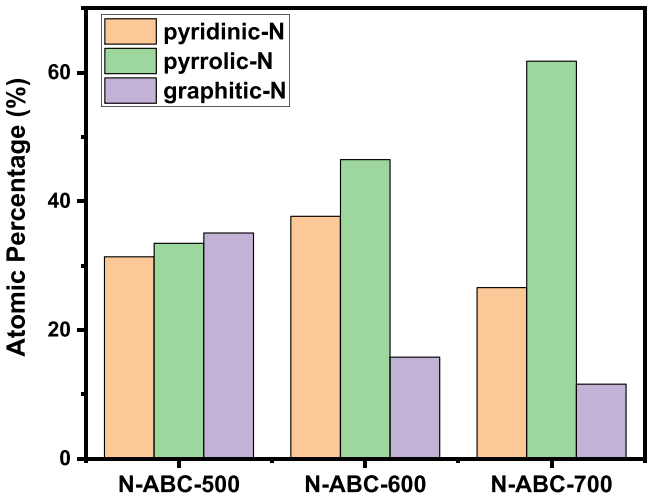


Fig. 10. Relative atomic percentages of the N-ABC supports, determined by XPS. Adapted from the surface analysis reported in reference [9].

through the dry impregnation method, utilizing ammonium ferric citrate as a precursor. The obtained samples were labeled as Fe/NCNT, and compared to iron supported on oxygen-modified carbon nanotubes catalysts, which denoted as Fe/OCNT and iron supported on silica catalysts, dented Fe/SiO_2. XANES analysis showed that the reduction of iron oxide on nitrogen-doped CNTs was much more effective than on the other two supports (O-CNTs and SiO_2) [68]. In addition, the H_2-TPR analyses revealed that the reduction of iron oxide nanoparticles on nitrogen-doped carbon nanotubes (NCNTs) was more facile compared to those of oxygen-doped carbon nanotubes (OCNTs) and SiO_2, which demonstrated a higher resistance to the reduction. Recently, Sun et al. [69]. studied the effect of nitrogen doping on the bimetallic catalysts via mesoporous carbon sphere-supported Ru-Cu (Ru-Cu/NMCN) in the catalytic CO_2 methanation. The optimal Ru/Cu molar ratio for the highest catalytic activity was 1/10. That optimized Ru-Cu/NMCN catalyst exhibited high CO_2 conversion (53 %) and CH_4 selectivity (88 %) at 500 °C, which is attributed to the synergistic effect and the N-doping.

the few reported studies on the impact of nitrogen doping into the carbon-based materials, used in CO_2 methanation catalysts reveal the crucial role of nitrogen in enhancing catalytic activity, selectivity, and stability. Utilizing carbon supports such as nanotubes, nanofibers, and mesoporous spheres doped with nitrogen and various metal nanoparticles (e.g., Ru, Ni, Co, Fe) leads to improved metal dispersion and enhanced metal-support interaction. Moreover, the type and content of nitrogen species on carbon supports influence the catalytic performance, particularly pyridinic-N species. Overall, nitrogen-doped carbon materials could be considered as promising supports for the CO_2 methanation catalysts, as shown in Table 7 which presents the collected results of the reported N-doped carbonaceous catalysts, confirming that the nitrogen-doped carbon materials are promising in the CO_2 methanation process.

10. Conclusions

In this review, we discussed the various carbonaceous materials, which were reported as supports for the CO_2 methanation catalysts, such as carbon nanotubes (CNTs), graphene, and biochar. The preparation methods and promoters are key steps for the fabrication of a robust catalyst. The synthesis technique should offer a perfect metal-support interaction. In addition, it should guarantee that the active sites of the main metal are easily accessible and not covered or blocked by the promoter. Besides, the metal loading has a significant role in the successful synthesis of the catalyst, as it should be sufficient to achieve maximum efficiency. However, increasing the metal content may result in agglomeration and/or bigger particle sizes, leading to less catalytic performance. It is worth noting that the calcination temperature affects the porosity, metal particle size, and metal support interaction. It is reported that increasing the calcination temperature of CNTs-supported Ni catalysts by more than 400 °C results in higher porosity, bigger particle sizes, and weaker metal support interaction, attributed to the electronic and geometric effects.

Chemical activation of the carbonaceous support, using activating agent such as nitric acid or sulfuric acid, together with physical activation by heating in nitrogen can enable us to modify the carbon to obtain mesoporous carbon with a high surface area and porous structure, resulting in improved adsorption capacity, and accordingly high catalytic performance. The activation energy can be also modified by addition of promoters, such as cerium, which can make changes to the electronic structure of the reactants, having them more reactive. The addition of cerium to some Ni catalysts could decrease the activation energy from 84.8 to 13.1 kJ/mol. The reported gas hourly space velocity (GHSV) varied intelligibly, as every experimental setup has its own optimal GHSV. However, increasing the GHSV may cause a decrease in the residence time, resulting in less catalytic activity. The GHSV not only affects the carbon dioxide conversion but it also has an impact on the methane selectivity. For instance, it is reported that increasing the GHSV from 60,000 to 120,000 (mL/g_{cat}.h) resulted in a decrease in the carbon dioxide conversion from 80 % to 73 % with a slight decrease in the methane selectivity from 99 % to 94 %.

The effect of nitrogen doping on the carbon-supported catalysts was rarely reported in the CO_2 methanation. However, the reported results confirm that nitrogen doping can enhance the basicity and reducibility, leading to higher catalytic activity. It is also worth noting that there are

Table 7
Collected results for the N-doped catalysts, reported in the CO_2 methanation.

Metal	Carbon Support	Metal Loading (wt %)	Preparation method	Reaction conditions	CO_2 conversion (%)	CH_4 selectivity (%)	CH_4 Yield (%)	Ref.
Fe	Nitrogen doped Carbon nanotube	38.3	Dry impregnation	360 ∘C 25 bar H_2/CO_2=3	25.2 %	39.9 %	/	[68]
Ru	Nitrogen-Doped Carbon Nanofibers	5	incipient wetness impregnation	350∘C H_2/CO_2=3	66 %	99 %	/	[64]
Ru	N-doped biochar (Pinus sylvestris)	3	wet impregnation method	380 °C 10 bar H_2:CO_2 =4	93.8 %	99.7 %	/	[9]
Ni	Nitrogen-Doped Carbon Nanofibers	10.7	wet impregnation	360 °C H_2:CO_2= 6	94 %	98 %	/	[32]
Ni	Nitrogen-doped CNTs	30	impregnation	340°C	50 %	95 %	/	[28]
Ni	Nitrogen-doped CNTs	15	Wet impregnation	400°C	81.2 %	92 %	80.6 %	[30]
Ru-Cu	Nitrogen doped mesoporous-carbon	1:10 Ru:Cu (molar ratio)	Wet impregnation	500°C	53 %	88 %	/	[69]

no reported theoretical studies on the carbon-supported catalysts used in CO_2 methanation. Therefore, computational studies are urgently needed to help explain if carbon supports contribute to the most argued topic about the activation routes of CO_2 and CO (hydrogenation or direct dissociation) and the chances of forming CO* as an intermediate. Computational chemistry will help to understand the CO_2 reaction with hydrogen on the catalyst support, understand the difference of the process on different crystal facets, solve some mechanisms under debate, and offer the opportunity to design new nanocatalysts to achieve not only high conversion and selectivity but also high stability and low cost [70–72]. Carbon allotrope supports will challenge the computational catalysis because they might have defects, nitrogen or sulfur sites to be considered on top of the immobilized nanocatalyst itself, in the reaction pathways to methane.

CRediT authorship contribution statement

Yahia H. Ahmad: Writing – review & editing. **Ahmed Gamal:** Writing – original draft, Conceptualization. **Mengqi Tang:** Writing – review & editing. **Kenneth I. Ozoemena:** Validation. **Aboubakr M. Abdullah:** Supervision. **Mohamed M. Chehimi:** Methodology. **Khouloud Jlassi:** Writing – review & editing, Validation, Supervision, Funding acquisition. **Siham Y. Alqaradawi:** Validation.

Declaration of Competing Interest

The authors declare no conflict of interest that could have appeared to influence the presented work. KHOULOUD JLASSI, MOHAMMED CHEHIMI, ABOUBAKR ABDULLAH, Kenneth I. Ozoemena reports financial support was provided by Qatar University. JLASSI KHOULOUD reports a relationship with Qatar University that includes: employment. NA If there are other authors, they declare that they have no known competing financial interests or personal relationships that could have appeared to influence the work reported in this paper.

Data availability

The data that has been used is confidential.

Acknowledgments

This work was supported by (i) the Qatar Research Development and Innovation Council (QRDI, a member of the Qatar Foundation, through the Academic Research Grant (ARG01-0530-230416), (ii) Qatar University through an International Research Collaboration Co-Fund grant, IRCC-2023-015, and (iii) South Africa's National Foundation of Research (NRF) through the DSI-NRF-Wits SARChI Chair in Materials Electrochemistry and Energy Technologies (MEET) (UID No.: 132739).

References

[1] A. Gamal, K. Eid, A.M. Abdullah, Engineering of Pt-based nanostructures for efficient dry (CO2) reforming: strategy and mechanism for rich-hydrogen production, Int. J. Hydrogen Energy 47 (9) (2022) 5901–5928.
[2] Y. Pan, X. Han, X. Chang, H. Zhang, X. Zi, Z. Hao, J. Chen, Z. Lin, M. Li, X. Ma, Enhanced Low-Temperature CO2 Methanation over Bimetallic Ni–Ru Catalysts, Industrial & Engineering Chemistry Research (2023).
[3] L. Song, H. Wang, S. Wang, Z. Qu, Dual-site activation of H2 over Cu/ZnAl2O4 boosting CO2 hydrogenation to methanol, Appl. Catal. B: Environ. 322 (2023) 122137.
[4] A. Sardar, D. Kumar, A. Gamal, M.M. Khader, E.-N. Muftah, Metal-silica nanocomposites prepared through a single step solution combustion synthesis (scs), Google Pat. (2022).
[5] P. Riani, E. Spennati, M.V. Garcia, V.S. Escribano, G. Busca, G. Garbarino, Ni/Al2O3 catalysts for CO2 methanation: effect of silica and nickel loading, Int. J. Hydrogen Energy (2023).
[6] K. Eid, A. Gamal, A.M. Abdullah, Graphitic carbon nitride-based nanostructures as emergent catalysts for carbon monoxide (CO) oxidation, Green Chem. 25 (4) (2023) 1276–1310.
[7] J.L. Figueiredo, M.F. Pereira, M.M. Freitas, J.J. Órfão, Characterization of active sites on carbon catalysts, Ind. Eng. Chem. Res. 46 (12) (2007) 4110–4115.
[8] L. Shen, J. Xu, M. Zhu, Y.-F. Han, Essential role of the support for nickel-based CO2 methanation catalysts, ACS Catal. 10 (24) (2020) 14581–14591.
[9] X. Wang, Y. Liu, L. Zhu, Y. Li, K. Wang, K. Qiu, N. Tippayawong, P. Aggarangsi, P. Reubroycharoen, S. Wang, Biomass derived N-doped biochar as efficient catalyst supports for CO2 methanation, J. CO2 Util. 34 (2019) 733–741.
[10] Y. Xie, J. Wen, Z. Li, J. Chen, Q. Zhang, P. Ning, Y. Chen, J. Hao, Progress in reaction mechanisms and catalyst development of ceria-based catalysts for low-temperature CO 2 methanation, Green. Chem. 25 (1) (2023) 130–152.
[11] B. Miao, S.S.K. Ma, X. Wang, H. Su, S.H. Chan, Catalysis mechanisms of CO 2 and CO methanation, Catal. Sci. Technol. 6 (12) (2016) 4048–4058.
[12] Z. Liu, X. Gao, B. Liu, Q. Ma, T.-s. Zhao, J. Zhang, Recent advances in thermal catalytic CO2 methanation on hydrotalcite-derived catalysts, Fuel 321 (2022) 124115.
[13] L. Li, W. Zeng, M. Song, X. Wu, G. Li, C. Hu, Research progress and reaction mechanism of CO2 methanation over Ni-based catalysts at low temperature: a review, Catalysts 12 (2) (2022) 244.
[14] W.J. Lee, C. Li, H. Prajitno, J. Yoo, J. Patel, Y. Yang, S. Lim, Recent trend in thermal catalytic low temperature CO2 methanation: a critical review, Catal. Today 368 (2021) 2–19.
[15] P. Frontera, A. Macario, M. Ferraro, P. Antonucci, Supported catalysts for CO2 methanation: a review, Catalysts 7 (2) (2017) 59.
[16] C. Lv, L. Xu, M. Chen, Y. Cui, X. Wen, Y. Li, C.E. Wu, B. Yang, Z. Miao, X. Hu, Recent progresses in constructing the highly efficient Ni based catalysts with advanced low-temperature activity toward CO2 methanation, Front. Chem. 8 (2020) 269.
[17] E. Furimsky, CO2 hydrogenation to methanol and methane over carbon-supported catalysts, Ind. Eng. Chem. Res. 59 (35) (2020) 15393–15423.
[18] A.I. Tsiotsias, N.D. Charisiou, I.V. Yentekakis, M.A. Goula, Bimetallic Ni-based catalysts for CO2 methanation: a review, Nanomaterials 11 (1) (2020) 28.
[19] A.I. Tsiotsias, N.D. Charisiou, I.V. Yentekakis, M.A. Goula, The role of alkali and alkaline earth metals in the CO2 methanation reaction and the combined capture and methanation of CO2, Catalysts 10 (7) (2020) 812.
[20] M. Younas, L. Loong Kong, M.J. Bashir, H. Nadeem, A. Shehzad, S. Sethupathi, Recent advancements, fundamental challenges, and opportunities in catalytic methanation of CO2, Energy Fuels 30 (11) (2016) 8815–8831.
[21] M. Tang, A. Gamal, A.K. Bhakta, K. Jlassi, A.M. Abdullah, M.M. Chehimi, Carbon Dioxide Methanation Enabled by Biochar-Nanocatalyst Composite Materials: A Mini-Review, Catalysts 14 (2) (2024) 155.
[22] S. Rathinavel, K. Priyadharshini, D. Panda, A review on carbon nanotube: An overview of synthesis, properties, functionalization, characterization, and the application, Mater. Sci. Eng.: B 268 (2021) 115095.
[23] X. Pan, X. Bao, The effects of confinement inside carbon nanotubes on catalysis, Acc. Chem. Res. 44 (8) (2011) 553–562.
[24] N. Behabtu, C.C. Young, D.E. Tsentalovich, O. Kleinerman, X. Wang, A.W. Ma, E. A. Bengio, R.F. Ter Waarbeek, J.J. De Jong, R.E. Hoogerwerf, Strong, light, multifunctional fibers of carbon nanotubes with ultrahigh conductivity, science 339 (6116) (2013) 182–186.
[25] E. Suslova, S. Chernyak, A. Egorov, S. Savilov, V. Lunin, CO 2 hydrogenation over cobalt-containing catalysts, Kinet. Catal. 56 (2015) 646–654.
[26] W. Wang, W. Chu, N. Wang, W. Yang, C. Jiang, Mesoporous nickel catalyst supported on multi-walled carbon nanotubes for carbon dioxide methanation, Int. J. Hydrog. Energy 41 (2) (2016) 967–975.
[27] M. Romero-Sáez, A. Dongil, N. Benito, R. Espinoza-González, N. Escalona, F. Gracia, CO2 methanation over nickel-ZrO2 catalyst supported on carbon nanotubes: A comparison between two impregnation strategies, Appl. Catal. B: Environ. 237 (2018) 817–825.
[28] J. Gödde, M. Merko, W. Xia, M. Muhler, Nickel nanoparticles supported on nitrogen–doped carbon nanotubes are a highly active, selective and stable CO2 methanation catalyst, J. Energy Chem. 54 (2021) 323–331.
[29] AG. Dyachenko, O.V. Ischenko, O.V. Prygunova, V.E. Diyuk, G.G. Tsapyuk, S. V. Gaidai, A.V. Yatsymyrskyi, T.M. Zakharova, E.O. Kostyrko, Ni–Fe, Co–Fe, and Co–Ni nanocomposites based on carbon nanotubes in the reaction of CO2 methanation, Mol. Cryst. Liq. Cryst. 720 (1) (2021) 38–46.
[30] L.P. Gonçalves, M. Meledina, A. Meledin, D.Y. Petrovykh, J.P. Sousa, O.S.G. Soares, Y.V. Kolen'ko, M.F.R. Pereira, Understanding the importance of N− doping for CNT-supported Ni catalysts for CO2 methanation, Carbon 195 (2022) 35–43.
[31] J. Li, Y. Zhou, X. Xiao, W. Wang, N. Wang, W. Qian, W. Chu, Regulation of Ni–CNT interaction on Mn-promoted nickel nanocatalysts supported on oxygenated CNTs for CO2 selective hydrogenation, ACS Appl. Mater. Interfaces 10 (48) (2018) 41224–41236.
[32] W. Wang, C. Duong-Viet, H. Ba, W. Baaziz, G. Tuci, S. Caporali, L. Nguyen-Dinh, O. Ersen, G. Giambastiani, C. Pham-Huu, Nickel nanoparticles decorated nitrogen-doped carbon nanotubes (Ni/N-CNT); a robust catalyst for the efficient and selective CO2 methanation, ACS Appl. Energy Mater. 2 (2) (2018) 1111–1120.
[33] R. Wang, Z. Wu, C. Chen, Z. Qin, H. Zhu, G. Wang, H. Wang, C. Wu, W. Dong, W. Fan, Graphene-supported Au–Pd bimetallic nanoparticles with excellent catalytic performance in selective oxidation of methanol to methyl formate, Chem. Commun. 49 (74) (2013) 8250–8252.
[34] C.-C. Yeh, D.-H. Chen, Ni/reduced graphene oxide nanocomposite as a magnetically recoverable catalyst with near infrared photothermally enhanced activity, Appl. Catal. B: Environ. 150 (2014) 298–304.
[35] Y. Krisnandi, I. Abdullah, I. Prabawanta, M. Handayani, In-situ hydrothermal synthesis of nickel nanoparticle/reduced graphene oxides as catalyst on CO2 methanation, in: AIP Conference Proceedings, AIP Publishing, 2020.

[36] H. Ma, K. Ma, J. Ji, S. Tang, C. Liu, W. Jiang, H. Yue, B. Liang, Graphene intercalated Ni-SiO2/GO-Ni-foam catalyst with enhanced reactivity and heat-transfer for CO2 methanation, Chem. Eng. Sci. 194 (2019) 10–21.
[37] J. Wu, Z. Jin, B. Wang, Y. Han, Y. Xu, Z. Liang, Z. Wang, Nickel nanoparticles encapsulated in microporous graphenelike carbon (Ni@ MGC) as catalysts for CO2 methanation, Ind. Eng. Chem. Res. 58 (45) (2019) 20536–20542.
[38] F. Hu, S. Tong, K. Lu, C.-M. Chen, F.-Y. Su, J. Zhou, Z.-H. Lu, X. Wang, G. Feng, R. Zhang, Reduced graphene oxide supported Ni-Ce catalysts for CO2 methanation: The support and ceria promotion effects, J. CO2 Util. 34 (2019) 676–687.
[39] N.D. Mohd Ridzuan, M.S. Shaharun, K.M. Lee, I. Ud Din, P. Puspitasari, Influence of nickel loading on reduced graphene oxide-based nickel catalysts for the hydrogenation of carbon dioxide to methane, Catalysts 10 (5) (2020) 471.
[40] F. Hu, X. Chen, Z. Tu, Z.-H. Lu, G. Feng, R. Zhang, Graphene aerogel supported Ni for CO2 hydrogenation to methane, Ind. Eng. Chem. Res. 60 (33) (2021) 12235–12243.
[41] A. Mohanty, C.D. Viet, A.-C. Roger, A. Adam, D. Mertz, W. Baaziz, I. Janowska, Structural impact of carbon nanofibers/few-layer-graphene substrate decorated with Ni for CO2 methanation via inductive heating, Appl. Catal. B: Environ. 298 (2021) 120589.
[42] D. Méndez-Mateos, V.L. Barrio, J.M. Requies, M. Gil-Calvo, Graphene-based versus alumina supports on CO2 methanation using lanthanum-promoted nickel catalysts, Environ. Sci. Pollut. Res. (2023) 1–25.
[43] N.L. Visser, O. Daoura, P.N. Plessow, L.C. Smulders, J.W. de Rijk, J.A. Stewart, B. D. Vandegehuchte, F. Studt, J.E. van der Hoeven, P.E. de Jongh, Particle size effects of carbon supported nickel nanoparticles for high pressure CO2 methanation, ChemCatChem 14 (22) (2022) e202200665.
[44] X. Wang, M. Yang, X. Zhu, L. Zhu, S. Wang, Experimental study and life cycle assessment of CO2 methanation over biochar supported catalysts, Appl. Energy 280 (2020) 115919.
[45] C. Di Stasi, S. Renda, G. Greco, B. González, V. Palma, J.J. Manyà, Wheat-straw-derived activated biochar as a renewable support of Ni-CeO2 catalysts for CO2 methanation, Sustainability 13 (16) (2021) 8939.
[46] X. Li, Y. Wang, G. Zhang, W. Sun, Y. Bai, L. Zheng, X. Han, L. Wu, Influence of Mg-promoted Ni-based catalyst supported on coconut shell carbon for CO2 methanation, ChemistrySelect 4 (3) (2019) 838–845.
[47] S. Renda, C. Di Stasi, J.J. Manyà, V. Palma, Biochar as support in catalytic CO2 methanation: Enhancing effect of CeO2 addition, J. CO2 Util. 53 (2021) 101740.
[48] P. Tarifa, C. Megías-Sayago, F. Cazañ̃a, M. González-Martín, N. Latorre, E. Romeo, J.J. Delgado, A. Monzón, Highly active Ce-and Mg-promoted Ni catalysts supported on cellulose-derived carbon for low-temperature CO2 methanation, Energy Fuels 35 (21) (2021) 17212–17224.
[49] F. Mateus, P. Teixeira, J.M. Lopes, C. Henriques, C. Bacariza, CO2 Methanation on Ni Catalysts Supported over Activated Carbons Derived from Cork Waste, Energy & Fuels (2023).
[50] A. Gamal, M. Tang, A.K. Bhakta, Y. Snoussi, A.M. Khalil, K. Jlassi, M.M. Chehimi, A.M.A. Ali, CO2 methanation using sugarcane bagasse biochar/nickel sustainable catalysts, Mater. Today Sustain. (2023) 100627.
[51] M. Tang, Y. Snoussi, A.K. Bhakta, M. El Garah, A.M. Khalil, S. Ammar, M. M. Chehimi, Unusual, hierarchically structured composite of sugarcane pulp bagasse biochar loaded with Cu/Ni bimetallic nanoparticles for dye removal, Environ. Res. (2023) 116232.
[52] K. Stangeland, H. Li, Z. Yu, CO 2 hydrogenation to methanol: the structure–activity relationships of different catalyst systems, Energy Ecol. Environ. 5 (2020) 272–285.
[53] Y. Feng, W. Yang, W. Chu, Effect of Ca modification on the catalytic performance of Ni/AC for CO2 methanation, Integr. Ferroelectr. 172 (1) (2016) 40–48.
[54] L.P. Gonçalves, J. Mielby, O.S.G. Soares, J.P. Sousa, D.Y. Petrovykh, O.I. Lebedev, M.F.R. Pereira, S. Kegnæs, Y.V. Kolen'ko, In situ investigation of the CO2 methanation on carbon/ceria-supported Ni catalysts using modulation-excitation DRIFTS, Appl. Catal. B: Environ. 312 (2022) 121376.
[55] W. Wang, C. Duong-Viet, L. Truong-Phuoc, J.-M. Nhut, L. Vidal, C. Pham-Huu, Activated carbon supported nickel catalyst for selective CO2 hydrogenation to synthetic methane under contactless induction heating, Catal. Today 418 (2023) 114073.
[56] V. Jiménez, P. Sánchez, P. Panagiotopoulou, J.L. Valverde, A. Romero, Methanation of CO, CO2 and selective methanation of CO, in mixtures of CO and CO2, over ruthenium carbon nanofibers catalysts, Appl. Catal. A: Gen. 390 (1-2) (2010) 35–44.
[57] S. Gaidai, V. Gryn'ko, M. Zhludenko, A. Dyachenko, V. Tkach, O. Ishchenko, Activity of carbon-fiber-supported Fe–Co catalysts in the CO 2 methanation reaction, J. Superhard Mater. 39 (2017) 122–128.
[58] C.S. Sharma, H. Katepalli, A. Sharma, M. Madou, Fabrication and electrical conductivity of suspended carbon nanofiber arrays, Carbon 49 (5) (2011) 1727–1732.
[59] B. Jurca, L. Peng, A. Primo, A. Gordillo, A. Dhakshinamoorthy, V.I. Parvulescu, H. García, Promotional effects on the catalytic activity of Co-Fe alloy supported on graphitic carbon for CO2 hydrogenation, Nanomaterials 12 (18) (2022) 3220.
[60] K.N. Ahmad, W.N.R.W. Isahak, M.I. Rosli, M.R. Yusop, M.B. Kassim, M.A. Yarmo, Rare earth metal doped nickel catalysts supported on exfoliated graphitic carbon nitride for highly selective CO and CO2 methanation, Appl. Surf. Sci. 571 (2022) 151321.
[61] M.-J. Kim, J.-R. Youn, H.J. Kim, M.W. Seo, D. Lee, K.S. Go, K.B. Lee, S.G. Jeon, Effect of surface properties controlled by Ce addition on CO2 methanation over Ni/Ce/Al2O3 catalyst, Int. J. Hydrogen Energy 45 (46) (2020) 24595–24603.
[62] Y.H. Lee, J.Y. Ahn, D.D. Nguyen, S.W. Chang, S.S. Kim, S.M. Lee, Role of oxide support in Ni based catalysts for CO 2 methanation, RSC Adv. 11 (29) (2021) 17648–17657.
[63] S. Kim, Y. Yang, R. Lippi, H. Choi, S. Kim, D. Chun, H. Im, S. Lee, J. Yoo, Low-rank coal supported Ni catalysts for CO2 methanation, Energies 14 (8) (2021) 2040.
[64] L. Roldán, Y. Marco, E. García-Bordejé, Origin of the excellent performance of ru on nitrogen-doped carbon nanofibers for CO2 hydrogenation to CH4, ChemSusChem 10 (6) (2017) 1139–1144.
[65] C. Hu, L. Dai, Doping of carbon materials for metal-free electrocatalysis, Adv. Mater. 31 (7) (2019) 1804672.
[66] S. Majeed, J. Zhao, L. Zhang, S. Anjum, Z. Liu, G. Xu, Synthesis and electrochemical applications of nitrogen-doped carbon nanomaterials, Nanotechnol. Rev. 2 (6) (2013) 615–635.
[67] D. Wei, Y. Liu, Y. Wang, H. Zhang, L. Huang, G. Yu, Synthesis of N-doped graphene by chemical vapor deposition and its electrical properties, Nano Lett. 9 (5) (2009) 1752–1758.
[68] L.M. Chew, P. Kangvansura, H. Ruland, H.J. Schulte, C. Somsen, W. Xia, G. Eggeler, A. Worayingyong, M. Muhler, Effect of nitrogen doping on the reducibility, activity and selectivity of carbon nanotube-supported iron catalysts applied in CO2 hydrogenation, Appl. Catal. A: Gen. 482 (2014) 163–170.
[69] H. Sun, R. Tang, X. Zhang, S. Zou, Y. Shi, K. Chen, S. Sarina, J. Huang, RuCu bimetallic catalyst on N-doped mesoporous carbon for high-performance CO2 methanation, Carbon Capture Sci. Technol. 6 (2023) 100100.
[70] D. Cheng, F.R. Negreiros, E. Aprà, A. Fortunelli, Computational approaches to the chemical conversion of carbon dioxide, ChemSusChem 6 (6) (2013) 944–965.
[71] A. Álvarez, M. Borges, J.J. Corral-Pérez, J.G. Olcina, L. Hu, D. Cornu, R. Huang, D. Stoian, A. Urakawa, CO2 activation over catalytic surfaces, ChemPhysChem 18 (22) (2017) 3135–3141.
[72] C. Vogt, M. Monai, E.B. Sterk, J. Palle, A.E. Melcherts, B. Zijlstra, E. Groeneveld, P. H. Berben, J.M. Boereboom, E.J. Hensen, Understanding carbon dioxide activation and carbon–carbon coupling over nickel, Nat. Commun. 10 (1) (2019) 5330.